



HAL
open science

Individual and population approaches for calibrating division rates in population dynamics: Application to the bacterial cell cycle

Marie Doumic, Marc Hoffmann

► To cite this version:

Marie Doumic, Marc Hoffmann. Individual and population approaches for calibrating division rates in population dynamics: Application to the bacterial cell cycle. *Modeling and Simulation for Collective Dynamics*, 40, WORLD SCIENTIFIC, pp.1-81, 2023, Lecture Notes Series, Institute for Mathematical Sciences, National University of Singapore, 10.1142/9789811266140_0001 . hal-03328781v2

HAL Id: hal-03328781

<https://hal.science/hal-03328781v2>

Submitted on 30 Dec 2022

HAL is a multi-disciplinary open access archive for the deposit and dissemination of scientific research documents, whether they are published or not. The documents may come from teaching and research institutions in France or abroad, or from public or private research centers.

L'archive ouverte pluridisciplinaire **HAL**, est destinée au dépôt et à la diffusion de documents scientifiques de niveau recherche, publiés ou non, émanant des établissements d'enseignement et de recherche français ou étrangers, des laboratoires publics ou privés.

**Individual and population approaches
for calibrating division rates in population dynamics:
Application to the bacterial cell cycle**

Marie Doumic and Marc Hoffmann

*Sorbonne Universités, Inria, UPMC Univ Paris 06
Lab. J.L. Lions UMR CNRS 7598, Paris, France
marie.doumic@inria.fr*

*University Paris-Dauphine, CEREMADE,
Place du Maréchal De Lattre de Tassigny, 75016 Paris, France
hoffmann@ceremade.dauphine.fr*

Modelling, analysing and inferring triggering mechanisms in population reproduction is fundamental in many biological applications. It is also an active and growing research domain in mathematical biology. In this chapter, we review the main results developed over the last decade for the estimation of the division rate in growing and dividing populations in a steady environment. These methods combine tools borrowed from PDE's and stochastic processes, with a certain view that emerges from mathematical statistics. A focus on the application to the bacterial cell division cycle provides a concrete presentation, and may help the reader to identify major new challenges in the field.

Keywords: cell division cycle, bacterial growth, inverse problem, nonparametric statistical inference, kernel density estimation, growth-fragmentation equation, growth-fragmentation process, renewal equation, renewal process, adder model, incremental model, asymptotic behaviour, long-term dynamics, eigenvalue problem, Malthusian parameter

Mathematics Subject Classification: 35R30, 92B05, 35Q62, 62G05

Contents

1	Introduction	2
1.1	Biological motivation	2
1.2	Outline of the chapter	5

1.3	First step: data analysis	7
1.4	Second step: making assumptions	11
2	Building models	13
2.1	Continuous-time branching processes	14
2.2	Random measures	17
2.3	Structured population equations	24
3	Model analysis: long-time behaviour	27
3.1	The renewal equation: a pedagogical example	28
3.2	The renewal process	36
3.3	The growth-fragmentation equation	38
3.4	Structured population equations and processes	45
4	Model calibration: statistical estimation of the division rate	46
4.1	Estimating an age-dependent division rate	47
4.1.1	Individual dynamics data	47
4.1.2	Population point data	54
4.2	Estimating a size-dependent division rate	57
4.2.1	Individual dynamics data	57
4.2.2	Population point data	62
4.3	Estimating an increment-dependent division rate	68
5	Application to experimental data	71
5.1	Guideline of a protocol	71
5.2	Some results	72
6	Perspectives and open questions	74
	References	75

1. Introduction

1.1. *Biological motivation*

The study of stochastic or deterministic population dynamics, their qualitative behaviour and the inference of their characteristics is an increasingly important research field, which gathers various mathematical approaches as well as application fields. It benefits from the huge advances in gathering data, so that it is today possible not only to write and study qualitative models but also to calibrate them and assess their relevance in a quantitative manner. This chapter aims at contributing to review some recent advances and remaining challenges in the field, through the lense of a specific application, namely the bacterial cell division cycle. Guided by this application, we propose here a kind of roadmap for the mathematician in order to tackle a genuinely applied problem, coming from contemporary biology.

How does a population grow?

Let us begin by describing the growth of a microcolony of bacteria, illustrated in the snapshots of Figure 1 : out of one rod-shaped *E. coli* bacterium, a colony rapidly emerges by the growth of each bacterium and its splitting into two daughter cells.

Nutrient being in large excess at this development stage, we can assume a steady environment. We also ignore the many fascinating questions arising from spatial considerations [1, 2, 3], and focus on the two fundamental mechanisms at stake: growth and division. We can go back and forth between the population and the individual view: how does the knowledge of the growth and division laws of the individual lead to the knowledge of the population growth law, and conversely, to which extent observations on the population can help us infer the individual laws?

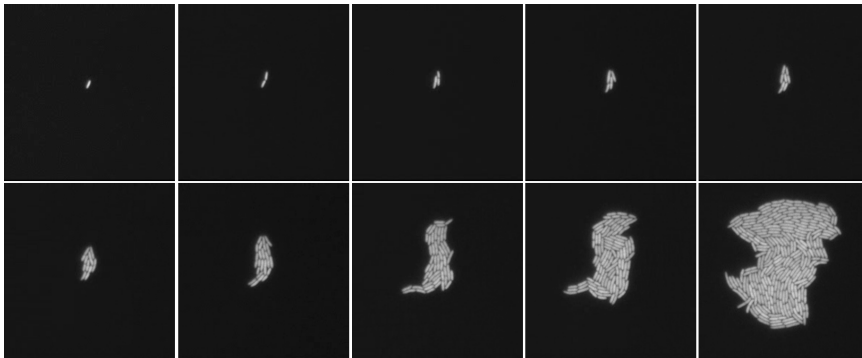


Fig. 1. From left to right and top to bottom: Successive snapshots of the video <https://doi.org/10.1371/journal.pbio.0030045.sv001>

How does a cell divide?

To follow more easily individual characteristics of the cells over many generations, a microfluidic liquid-culture device called "the mother machine" has been developed in the last decade with an increasing success [4, 5]. This is illustrated in Figure 2, a snapshot taken from the illustrating Movie S1, from [5]. The population is then reduced to independent lineages, but the two main mechanisms remain the same: growth and division. How do these two mechanisms coordinate each other? What triggers the bacterial

division? To answer such questions, many studies have deciphered complex intracellular mechanisms, see for instance the recent review [6], while others aim at inferring laws of growth and division out of the observation of population (as in Fig. 1) or lineages (as in Fig. 2) dynamics. This last approach, which could be named phenomenological rather than mechanistic, constitutes the guideline of this chapter, and could be summed-up by the problematic: How much information on triggering mechanisms of growth and division can be extracted from such data as in Figs. 1 and 2?

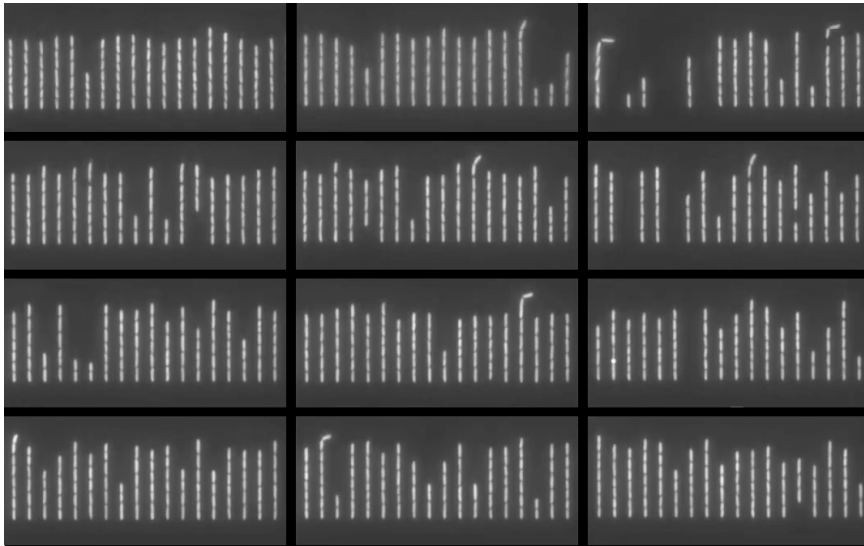


Fig. 2. From left to right and top to bottom: Snapshot of the video S1 of [5]. In each channel bacteria grow and divide while remaining aligned, pushing new born cells towards the exit.

Other applications

We follow here the application to cell division; however, many other are possible, such as polymer fragmentation [7, 8, 9], or mineral crushing [10], or yet other types of cell division cycles [11]. This would lead us too far for this chapter, but we believe that many ideas gathered here for bacteria may apply to other fields.

1.2. Outline of the chapter

To serve as an outline of the chapter, let us enumerate the main steps towards the formulation of laws of growth and division in a process which is rather circular than linear in practice. This – admittedly subjective – methodological guideline is quite general, and many readers should recognize their own approach to their own problem; we then explain and specify them when applied to growing and dividing populations, and, more precisely, to the bacterial cell division cycle.

- **Step 1) Preliminaries** - Sections 1.3 and 1.4
 - **Analyse data:** (or make the most of direct observations)
Biological data are often extremely rich, and only part of this richness is effectively analysed by experimenters, for instance through the use of averaged quantities rather than individual measurements. At the same time, the noise level is often very high, requiring an appropriate noise modelling approach. Mathematical methods at this first step are a combination of statistics, image analysis and interdisciplinary discussions between modellers and experimenters. This is carried out in our application case to bacterial growth and division in Section 1.3.
 - **Specify assumptions:** (or “model and simplify”)
The data analysis carried out at Step 1 should lead to two types of hypothesis: simplifying ones, *a priori* justified by statistical quantifiers and which should be *a posteriori* verified by sensitivity analysis; and modelling ones, guiding conjectures on the underlying laws, which should be challenged at the end of the procedure. This is carried out in Subsection 1.4.
- **Step 2) Build a model** - Section 2
The goal of Section 2 is to translate mathematically the assumptions done at Step 1. As suggested by the illustrations of Figs. 1 and 2, we may distinguish two types of models: individual-based and population models, leading to stochastic processes, branching trees, or integro-partial differential equations (PDEs).
- **Step 3) Analyse the model** - Section 3
The models analyses, carried out in Section 3, could seemingly be skipped to go directly to the conclusion by simulating the models

as best as possible, with available simulation packages, and comparing them to the data, using here again available fitting tools. We believe however that such approaches not only lack rigour but also risk missing enlightening information. Many success stories in many application domains could illustrate this general comment; in our very field, the cornerstone and foundation of the inverse problem solutions lies in the long-time asymptotics of the population models, as first described by B. Perthame and J. Zubelli [12]. For the polymer breakage application, not developed in this chapter, the use of time asymptotics as proved in [13] drastically simplified and justified the calibration of the fragmentation model [8, 9]. In Section 3, we thus review some of the main theoretical results which may prove useful for the following steps.

- **Step 4) Calibrate the model** - Section 4

We can do here the same remark as for Section 3: standard calibration methods are often applicable, reducing this step to the choice of up-to-date softwares. A main drawback would be the difficulty to assess the confidence we may have in the results obtained; above all, theoretical error estimation inform us on the quantity of information available in the data collected, thus able to inspire design of new experiments. We thus develop in Section 4 the inverse problem analyses carried out in the past decade for the different observation schemes, detailing some of the proofs in the illuminating example of the renewal model and in the "ideal mitosis" case, and reviewing the results obtained for more complex cases.

- **Step 5) Conclusion** - Section 5

At this stage, we have all the necessary tools on hand to confront a model to the data, and conclude on the validity on the modelling assumptions made at Step 2. In Section 5, a protocol to confront model to data is proposed and applied to experimental data for bacteria. It is however a step where many questions remain open, concerning the design and analysis of statistical tests as well as the formulation of new or more detailed models. It usually lead to bootstrapping the methodology by circulate another round from Steps 1 to 5.

1.3. First step: data analysis

To build models that can be compared to the data, a preliminary step consists in having clear ideas on what can be measured and how. We first distinguish two types of data collection and two observation schemes, and then give some examples of what can be directly obtained from the data.

Data description: two types of datasets

We have already shown in Figs 1 and 2 two modern experimental settings to observe bacterial growth. In these two settings, a picture is taken at given time intervals - typically here, every 1 to 5 min - giving access, through image analysis, not only to time-dependent (noisy) samples of sizes but also to genealogical data and to the knowledge of the time elapsed since birth, of size dimensions at birth and of size dimensions at division, and of the ratio between the mother cell size at division and the offspring sizes. In the sequel, we call such cases *individual dynamics data*, meaning that some knowledge about the growth and division processes may be directly inferred from the data, where individual dynamics are collected.

However, there are other situations, for instance when *ex vivo* samples are collected, when only cheaper devices are available, or when the quantities of interest are not dynamically measured, or yet for other applications such as protein fibrils. In all these cases, the experimenter can only observe size distribution of particles of interest, taken at one or several time points, but without being able to follow each one so that no individual observation of growth or division may be done. In the sequel, we call such cases *population point data*, meaning that we have information on the population dynamics or on point individual data, but no access to individual dynamics.

As detailed in Section 4, each type of data collection raises different problems. Schematically, in the population point data, one has to choose a given model, and the estimation questions at stake are to determine which parameters may be inferred from the data and how precise this inference is. In the individual dynamics data, data are much richer and so are the questions to tackle: first, as for the population point data, estimate model parameters, and second, assess quantitatively how accurate the model is, evaluate to which extent it can be enriched without over-estimation, and compare it with other models.

Data description: genealogical observation vs. population observation

In the individual dynamics data cases, we have seen two distinct experimental settings: either we follow the overall population until a certain time, as in Fig. 1 - we call this case the *population case*, corresponding to $k = 2$ in the following, k being the number of children at division - or we follow only one given lineage, since at each division we keep observing one out of the two daughter cells - we call this case the *genealogical case*, corresponding to $k = 1$ in the following. As explained in Section 2, the mathematical model needs to adapt to these two cases, and so need the mathematical analysis and the model calibration.

At first sight, the population point data collection seems to apply only to the the population observation scheme ($k = 2$), taking sparse pictures of a population state at some times. However, it could be imagined that in a given genealogical observation experiment ($k = 1$) we are not able to determine when or where a cell divides; this will be the case for instance if the timesteps of observation are too large. It is thus also interesting to develop models and calibration methods for this seemingly strange but not unrealistic case.

For the population observation case $k = 2$, if the cells are in constant growth conditions (unlimited nutrient and space), the so-called Malthusian parameter characterises the exponential growth of the population. We denote it here λ , meaning that the population grows like $e^{\lambda t}$ - rigorous meanings of this statement are provided in Section 3. The Malthusian parameter can be measured in various ways for many different experimental conditions - as the total biomass increase for instance. Equivalently, biologists often refer to the doubling time T_2 of the population, with the immediate relation $T_2 = \frac{\ln(2)}{\lambda}$.

Data analysis: size distributions

To each observation scheme correspond different types of data and specific measurement noise. Let us here gather some of the most frequent information we can extract.

It is possible to extract size dimension distributions from the two types of data collection described above. For instance, for a given sample of n cells in a *E. coli* population, we measure their lengths at a given time t to obtain

$$(x_1(t), \dots, x_n(t)),$$

the width being considered roughly constant among cells. As a first approximation, we may assume that the observation is a n -drawn of a random vector

$$(X_1(t), \dots, X_n(t)),$$

where the random variables $X_i(t)$ are independent, with common distribution $\mu(t)$; this assumption is obviously not valid, since we ignore the underlying dependent structure. Yet, it may well happen – and this will be extensively discussed later – that the sample behaves approximately for certain linear statistics like an n -drawn of a common distribution [14]. In particular, we may at least expect the convergence of the empirical measure

$$\mu_n = \frac{1}{n} \sum_{k=1}^n \delta_{X_k(t)} \quad (1.1)$$

to $\mu(t)$ in a weak sense [15], possibly quantified by a distance like Wasserstein [16, 17] that metrizes weak convergence. Assuming that μ has a density, and using for instance histograms or adaptive kernel density estimators we may obtain a smooth estimate for the size distribution $\mu(t)$. This is treated at length in Section 4. Assuming moreover that $\mu(t) = \mu$ does not depend on time, an assumption that can (and will) be justified in some cases by the asymptotic analysis carried out in Section 3, also known in biology as cell size homeostasis, we may concatenate all data taken at all time to get larger samples. This is illustrated in Fig. 3 Right, where we have shown the length-distribution of cells taken at any time out of genealogical observation ($k = 1$, data from [5]) in blue and population observation in green ($k = 2$, data from [18]).

Data analysis: Individual dynamics data analysis

In the case of individual dynamics data collection, it is not only possible to extract size distribution but also much more. Let us list some of the information we can extract from such rich data.

To begin with, we can measure the cell age, *i.e.* the time elapsed since birth; or yet - let us mention it due to its recent importance in the field [20, 21, 22] - size increment, *i.e.* the difference between the size of the bacteria at the time considered and their size at birth. A similar process as seen above for size leads us to age or size increment distributions as illustrated in Fig. 3 Left. In the same vein, we can also select only dividing cells, measure their size, age, size increment at division, and estimate these

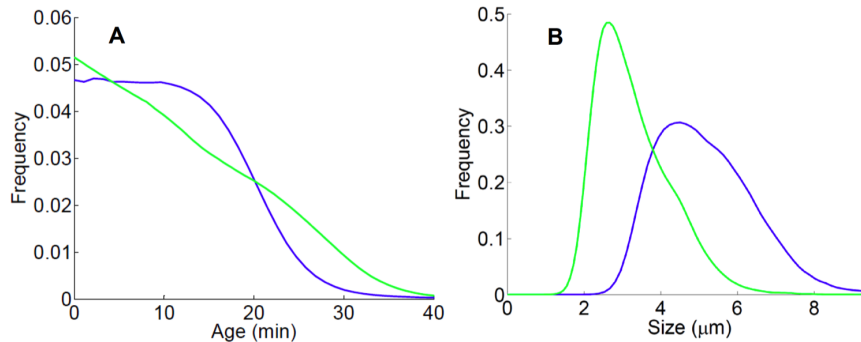


Fig. 3. **All cells distributions:** Kernel density estimation of age (Left) and length (Right) distributions obtained from sample images of genealogical observation (blue curves, data from [5]) and population observation (green curves, data from [18]), data taken at all time points. Figure taken from [19], Fig.1.

distributions: this is illustrated in Fig. 4. Finally, we can measure joint distributions, such as age-size or size-increment of size distributions: this is done in Fig. 5.

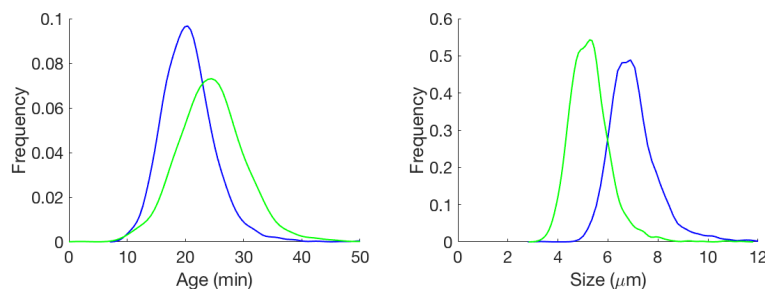


Fig. 4. **Dividing cells distributions:** Kernel density estimation of age (Left) and length (Right) distributions of dividing cells obtained from sample images of genealogical observation (blue curves, data from [5]) and population observation (green curves, data from [18]).

Being able to follow each cell means that we are also able to estimate individual growth rates. This is illustrated for one given cell in Fig. 6: measuring cell length and cell width every two minutes allows one to estimate its growth rate by curve fitting tools. On the right, we see width measure-

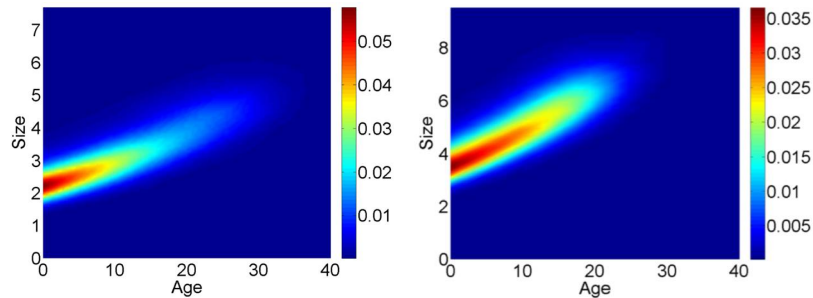


Fig. 5. Age-Size distributions for all cells. Left: population observation, data from [18], Right: genealogical observation, data from [5].

ments: it appears to remain constant up to measurement noise. On the left, we see the fit of the data with an exponential curve in red and with a linear curve in black: as studied in [19], and in accordance with previous studies, the exponential growth model, where we assume that the cell length evolves according to the law

$$\frac{dx}{dt} = \kappa x$$

for a certain rate $\kappa > 0$, fits the data very well - at least for the lengths where we have data, *i.e.* here for a range of sizes typical size between 0.3 to $5\mu\text{m}$.

But is this growth rate constant among all cells? As for the age or size distributions, once estimated for each cell, and assuming them independent (no heritability) and time-independent (no slowing down in growth due to lack of nutrient for instance), it is possible to study the distribution of growth rates. This is illustrated in Fig. 7, Left.

Concerning division, we already mentioned that it is possible to extract dividing cells distribution. But we have more information: for instance, it is possible to measure the ratio between daughter and mother cells. In our application setting, this is called the septum position, the *septum* being the boundary formed between the two dividing cells.

1.4. Second step: making assumptions

In the first step we have started to manipulate the data. It is clear that we could still get a lot of information from them: inheritance between mother

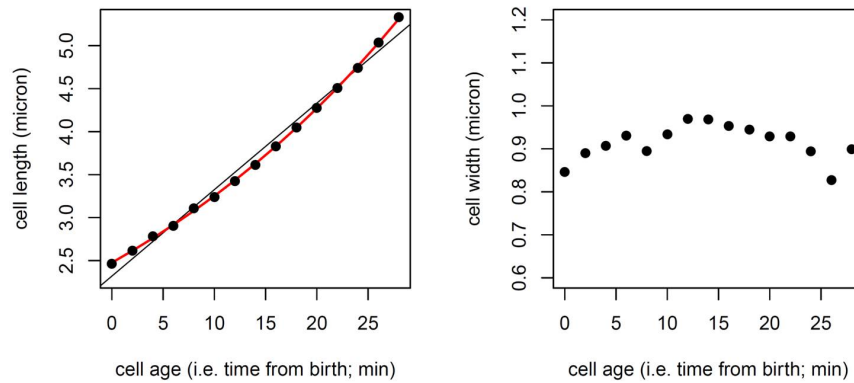


Fig. 6. *Single-cell growth rate analysis. Figure taken from [19] Figure 2. For a given cell, we measure its size dimensions - length on the right, width on the left - through time, and conclude to a good agreement of the exponential growth model $\frac{dx}{dt} = \kappa x$ for the length, and a constant width.*

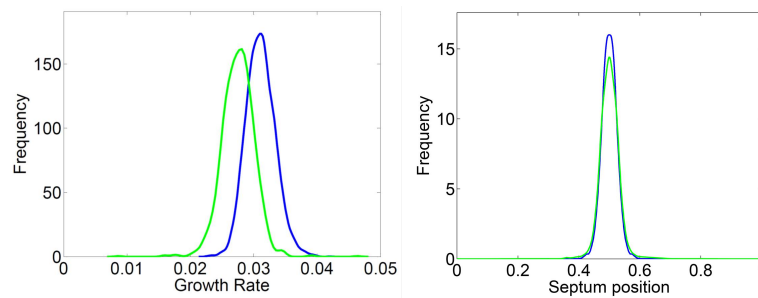


Fig. 7. *Growth rate in min^{-1} (Left) and daughter/mother ratio (Right) distributions. Blue curves: genealogical data from [5], Green curves: population data from [18]. Figure taken from Fig. S4 of [19].*

and daughter cells, distributions over time and not just aggregating all the time data, etc. Here and there, we already made two types of assumptions: model assumptions and simplifying assumptions. Let us gather them here, so that we will be ready to design mathematical models.

Simplifying assumptions can be made out of the direct observations done during the first step. In our application case, we list the following assumptions which will be used as a departure point for the calibration step, see Section 4.

- The daughter cell size at birth is half its mother cell size (Fig. 7 Right shows very little variability: we may neglect it first).
- All cells grow exponentially with the same growth rate κ (Fig. 7 Left shows some variability, that can be neglected in a first approximation).
- Space and nutrient consumption are infinite and do not influence growth and division (due to the experimental setting, this assumption may be verified by statistical analysis of time dynamics).

Model assumptions of course depend on the underlying application. They are the gateway to the third step and a way to formulate the vague question of the introduction: how to determine laws for growth and division? In our case, a central assumption, linked to the Markov property of our model, is the absence of memory between mother and daughter cells, *i.e.* we assume no heritability of the growth rate - see [23] for a thorough study of this question - and no heritability of the division features. Concerning growth, in the case of individual dynamics data collection, we have seen that we can formulate laws directly inferred from the data. This is not true concerning the law of division: the question "what triggers bacterial division?" remains unanswered by our data analysis step. We thus formulate the following modelling assumptions. They provide guidelines for all our subsequent models:

- A particle of age a and size x may divide with a division rate B depending on its age,
- a particle of age a and size x may divide with a division rate B depending on its size,
- a particle of size x and size at birth x_b may divide with a division rate B depending on its increment of size $x - x_b$,
- a particle of size x may divide with a division rate B depending on an auxiliary (and latent, *i.e.* unobserved) variable.

2. Building models

The preliminary steps sketched in Sections 1.3 and 1.4 allow one to have a clear idea on the necessary ingredients to translate mathematically the biological mechanisms to study. We list three apparently different approaches:

1. **Continuous-time branching processes:** the most direct and intuitive way is to model each cell of the population inside its genealogical tree, linking the parent to its offspring by a tree branch representing its

lifetime, each node representing a cell taken at birth or at division. We explain this model below in Section 2.1.

2. **Stochastic differential equations (SDE) via Poisson random measures:** this formalism is strictly equivalent to the building of the branching tree and consists in writing a stochastic differential equation satisfied by a random measure representing all the cells alive at a certain time. The advantage of writing this equation is that it is a very convenient way to link the stochastic model to the "deterministic" - or, more adequately, average - approach described in Section 2.3. This limit is rigorously proved in Section 2.2 in the pedagogical case of the renewal process, and we review results of the literature for other models.
3. **Integro-partial differential equations (PDE):** looking at a *large* population, or yet at the *average* behaviour of one or of a small number of individuals, we can write a balance equation satisfied by the concentration distribution of cells at time t , with given characteristics such as age, size, increment of size, etc: this gives rise to what is called a *structured population equation*, the term *structured* referring to this characteristic *trait* triggering growth, division, or more generally speaking evolution/change. This type of models is reviewed in Section 2.3.

Depending on the context or on the specific questions to be solved, one of the three above points of view may seem more advantageous, either from a technical or an interpretation point of view. The three approaches are closely related and sometimes equivalent. We next describe somehow their minimal mathematical features and their links.

2.1. *Continuous-time branching processes*

Continuous-time branching processes are classical objects, well documented in numerous textbooks and papers, see *e.g.* [24, 25, 26, 27] or [28, 29, 30, 31]. Ref. [32] is recommended for an efficient presentation of the topic.

The models we present here belong to the wide family of so-called "continuous-time branching trees", whose history dates back to 1873 [25] and knows continuous interest from ecologists as well as mathematicians, see *e.g.* [28] or for a specific and very recent example [33]. For the sake of simplicity, we stick here to the modelling and simplifying assumptions sketched above, so that our branching process is encoded in a binary tree: each node splits into exactly two branches. Using the Ulam-Neveu notation,

we define

$$\mathcal{U} := \bigcup_{n=0}^{\infty} \{0,1\}^n \quad \text{with } \{0,1\}^0 := \emptyset. \quad (2.1)$$

To each node $u \in \mathcal{U}$, we associate a cell with birth time b_u , size at birth

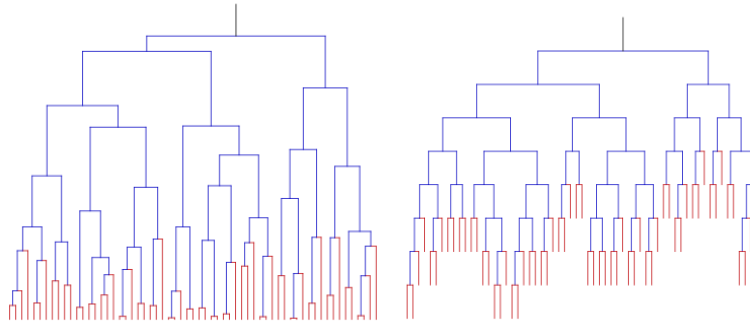


Fig. 8. *Simulation of a binary tree with. Left: the size of each segment represents the lifetime of an individual. Individuals alive at time t are represented in red. Right: genealogical representation of the same realisation of the tree. Figure taken from Fig. 1 of [14].*

ξ_u , lifetime ζ_u and increment of size since birth η_u . Assuming that the size growth is given by the growth rate $\tau(x)$ (in the sequel, we will often specify $\tau(x) = \kappa x$ for some common growth rate $\kappa > 0$), if $u^- \in \mathcal{U}$ denotes the parent of $u \in \mathcal{U}$, then the size at division is given by $\chi_u = X(\zeta_u, \xi_u)$ where $X(t, x)$ denotes the characteristic curve solution to the differential equation

$$\frac{dX(t, x)}{dt} = \tau(X(t, x)), \quad X(0, x) = x,$$

and we have, for a division probability kernel $b(\chi_u, dx)$

$$\xi_u \sim b(\chi_{u^-}, dx), \quad \eta_u = \chi_u - \xi_u = X(\zeta_u, \xi_u) - \xi_u.$$

In the specific case of exponential growth and diagonal kernel (equal mitosis, for which $b(\chi_u, dx) = \delta_{\frac{\chi_u}{2}}(dx)$), this gives

$$\xi_u = \frac{\chi_{u^-}}{2} = \frac{\xi_{u^-}}{2} \exp(\kappa \zeta_{u^-}), \quad \eta_u = \xi_u (\exp(\kappa \zeta_u) - 1).$$

We see that within such a formalism, it is straightforward to generalise our assumptions: for instance, the growth rate κ could be selected randomly at

birth, according to some probability law which could depend on the parent growth rate κ_{u^-} (or on some other trait of the mother). Another way to model unequal division is to write

$$\xi_{(u^-,0)} = \alpha \xi_{u^-} \exp(\kappa \zeta_{u^-}), \quad \xi_{(u^-,1)} = (1 - \alpha) \xi_{u^-} \exp(\kappa \zeta_{u^-}),$$

with $\alpha \in (0, 1)$ chosen randomly according to some probability distribution $b_0(d\alpha)$, symmetric in $\frac{1}{2}$. In such a case, the probability kernel b has a specific form, which is sometimes called *self-similar*, namely

$$b(y, x) = \frac{1}{y} b_0\left(\frac{x}{y}\right).$$

One last ingredient is still missing to have fully determined the tree: the distribution of the random time at which division occurs. Let us list the three examples discussed in the assumptions section above:

1. **The division depends on age:** this translates into the fact that given a division rate function

$$B : (0, \infty) \rightarrow [0, \infty), \quad \int_0^\infty B(s) ds = \infty,$$

the lifetime ζ_u is a random variable with distribution

$$\mathbb{P}(\zeta_u \in da) = B(a) e^{-\int_0^a B(s) ds} da.$$

Other said, we have

$$\mathbb{P}(\zeta_u \in (a, a + da) | \zeta_u \geq a) = B(a) da, \quad \mathbb{P}(\zeta_u \geq a) = \exp\left(-\int_0^a B(s) ds\right).$$

With this construction, the renewal process is simply embedded into a branching tree representation. See [14] for a study of a slight generalisation of this model. We notice that we can add other variables as the size and the increment of size, but they will have no influence on the tree.

2. **The division depends on size:** when the division is triggered by a size-dependent rate, and when the size grows at a rate $\tau(x)$, the division rate function now translates into the following properties

$$\mathbb{P}(\chi_u \in (x, x + dx) | \chi_u \geq x) = B(x) dx = \tau(x) B(x) dt,$$

$$\mathbb{P}(\chi_u \geq x | \xi_u) = \mathbb{1}_{\{x \geq \xi_u\}} \exp\left(-\int_{\xi_u}^x B(y) dy\right).$$

Notice that the age variable ζ_u , although well-defined, is a bit irrelevant in this context: this is due to the fact that we define an instantaneous rate $B(x) dx$ instead of defining a rate $B(x) dt$. Compared to previous mathematical papers [34, 35, 36, 37] etc., we simply substitute B by $B\tau$.

3. **The division depends on the increment of size since birth:** as for the renewal process, the increment is reset to zero at each division, however if the growth rate $\tau(x)$ is not constant it does not increase linearly with time, so that η_u is now characterised by

$$\mathbb{P}(\eta_u \in (z, z + dz) | \eta_u \geq z, \xi_u) = B(z)dz = B(z)\tau(\xi_u + z)dt,$$

$$\mathbb{P}(\eta_u \geq z) = \exp\left(-\int_0^z B(y)dy\right).$$

Indeed, for a size increment z we have a size since birth equal to $x = \xi_u + z$, and the size grows according to $\frac{dx}{dt} = d(\xi_u + z) = dz = \tau(x)dt$. When we embed the model in the time-continuous framework, we see that the lifetime does depend on size, contrarily to the renewal process, due to the fact that $dz \neq dt$ formally.

Given observational data, there are basically two ways of considering the tree: either we look at the process of structured cells *until a certain generation n* - along one branch chosen at random at each node (genealogical observation), or along chosen branches, or yet along all of them; alternatively, we look at the process *until a certain physical time* (population observation). In the first point of view, the physical time is not intrinsically important, contrarily to the second point of view, that we next adopt to describe the process via random measures.

2.2. Random measures

We consider the random process

$$X(t) = (X_1(t), X_2(t), \dots)$$

that describes the (ordered) sizes of the population at time t , or

$$A(t) = (A_1(t), A_2(t), \dots)$$

the (ordered) ages of the population at time t . Equivalently, we can define the random processes with values in finite-point measures on $(0, \infty)$ via

$$Z_t^{(a)} = \sum_{i=1}^{\infty} \delta_{A_i(t)}, \quad Z_t^{(x)} = \sum_{i=1}^{\infty} \delta_{X_i(t)}, \quad (2.2)$$

(the sum is finite but the total number of particles may be different for different values of t), that describe the population states, characterised by the structuring variables (here size, age, size increment and so on) at any given time t .

We can then look for a characterisation of the process $(Z_t^{(a)})_{t \geq 0}$ or $(Z_t^{(x)})_{t \geq 0}$ as via a stochastic evolution equation, here a measure-valued stochastic differential equation (SDE). In order to do so, we need a technical tool, namely the use of Poisson random measures.

Preliminaries: Poisson random measures

A convenient way to model scattered points or events through time and a state space is by means of a Poisson random measure. The notion and its properties are well documented in numerous textbooks, from stochastic geometry to stochastic calculus, see *e.g.* [38, 39, 40] and we briefly recall the essential and basic material needed here.

We start with a state space $\mathcal{X} \subset \mathbb{R}^d$ and we let μ be some sigma-finite measure on \mathcal{X} equipped with its Borel sigma-field. If $(x_i)_{i \in \mathcal{I}}$ is a countable family of elements of \mathcal{X} , the point measure N associated with $(x_i)_{i \in \mathcal{I}}$ is given by

$$N(dx) = \sum_{i \in \mathcal{I}} \delta_{x_i}(dx),$$

and its action on test functions $\varphi : \mathcal{X} \rightarrow \mathbb{R}$ is written as

$$\langle N, \varphi \rangle = \int_{\mathcal{X}} \varphi(x) N(dx) = \sum_{i \in \mathcal{I}} \varphi(x_i)$$

whenever the above sum is well-defined.

Definition 2.1: A random point measure N is a random Poisson measure on \mathcal{X} with intensity μ if

1. For every Borel set A , the random variable $N(A)$ has a Poisson distribution with parameter $\mu(A)$:

$$\mathbb{P}(N(A) = k) = e^{-\mu(A)} \frac{\mu(A)^k}{k!}, \quad k = 0, 1, \dots$$

2. For every countable family of Borel sets $(A_i)_{i \in \mathcal{I}}$ with $A_i \cap A_j = \emptyset$, if $i \neq j$, the random variables $(N(A_i))_{i \in \mathcal{I}}$ are independent.

Consider now a random measure N on $\mathcal{X} = [0, \infty) \times [0, \infty)$ with intensity $dt \otimes dx$. A first natural process that can be easily constructed from N is a so-called inhomogeneous Poisson process with intensity function $\lambda :$

$[0, \infty) \rightarrow [0, \infty)$. It models an event based process $(X_t)_{t \geq 0}$ that counts the events that occur between 0 and t according to the following two rules:

$\mathbb{P}(\text{an event occurs in } (t, t + dt) \mid \text{given the history up to time } t) = \lambda(t)dt$,

and $(X_t)_{t \geq 0}$ has independent increments: the random variables: $(X_{t_i+h_i} - X_{t_i})_{1 \leq i \leq n}$ are independent, for any family of disjoint sets $([t_i, t_i+h_i])_{1 \leq i \leq n}$. A possible construction is given by

$$X_t = \int_0^t \int_{[0, \infty)} \mathbb{1}_{\{u \leq \lambda(s)\}} N(ds, du).$$

To understand better the construction from a heuristic point of view, if $\lambda(s)$ is sufficiently smooth, for $s \in [t, t + dt]$, we can approximate $s \mapsto \lambda(s)$ by the constant function $s \mapsto \lambda(t)$ and thus obtain the chain of approximations

$$\begin{aligned} X_{t+dt} - X_t &= \int_t^{t+dt} \int_0^{\lambda(s)} N(ds, du) \\ &\approx \int_t^{t+dt} \int_0^{\lambda(t)} N(ds, du) = N([t, t + dt] \times [0, \lambda(t)]) \end{aligned}$$

which has a Poisson distribution of parameter $\lambda(t)dt$ since the intensity of N is $dt \otimes ds$. In particular, a standard Poisson process with parameter $\lambda > 0$ can be represented as $X_t = \int_0^t \int_{[0, \infty)} \mathbb{1}_{\{u \leq \lambda\}} N(ds, du)$. This is the basic ingredient to construct more elaborate jump models.

The simplest age model

We first prove the link between the deterministic and the stochastic model in the simplest age-dependent model: at time t , the age-structured cell population is described by the states (here the ages) of the living cells at time t , that we denote $(A_1(t), A_2(t), \dots, A_n(t), \dots)$ (given in the increasing order for instance), that we encode into the point measure

$$Z_t^{(a)} = Z_t(da) = \sum_{i=1}^{\infty} \delta_{A_i(t)}(da),$$

where the sum ranges from 1 to $\langle Z_t, \mathbb{1} \rangle$ and which is finite, as in (2.2). Assuming that the ages are ordered, we define the evaluation maps

$$a_i : Z_t \mapsto a_i(Z_t) = a_i \left(\sum_{j=1}^{\infty} \delta_{A_j(t)}(da) \right) = A_i(t).$$

Abusing notation slightly, we may identify $A_i(t)$ and $a_i(Z_t)$. We have a complete description of the stochastic dynamics of $Z_t = Z_t^{(k)}$ by means of a family of independent Poisson random measures $N_i(ds, d\vartheta)$, $i = 1, 2, \dots$ with intensity $ds \otimes d\vartheta$ on $[0, \infty) \times [0, \infty)$. It is given by the stochastic evolution equations, for $k = 1, 2$:

$$\begin{aligned} Z_t^{(k)} &= \tau_t Z_0 \\ &+ \int_0^t \sum_{i \leq \langle Z_{s-}^{(k)}, \mathbb{1} \rangle} \int_0^\infty (k\delta_{t-s} - \delta_{a_i(Z_{s-}^{(k)})+t-s}) \mathbb{1}_{\{\vartheta \leq B(a_i(Z_{s-}^{(k)}))\}} N_i(ds, d\vartheta), \end{aligned} \quad (2.3)$$

where

$$Z_0^{(k)} = \sum_{i=1}^{\langle Z_0^{(k)}, \mathbb{1} \rangle} \delta_{A_i(0)}$$

is an initial age distribution and

$$\tau_t Z_0^{(k)} = \sum_{i=1}^{\langle Z_0^{(k)}, \mathbb{1} \rangle} \delta_{A_i(0)+t}.$$

We have $k = 1$ for the genealogical observation case, where only one daughter cell is kept at each division, and $k = 2$ for the population observation case.

We may interpret (2.3) as follows: at time t the term $\tau_t Z_0^{(k)}$ accounts for the initial population that has aged by the amount t . This term must be corrected by:

- adding the ages of newborn cells. This is done as follows: a division event is run according to the rate $B(a_i(Z_{s-}^{(k)}))$, where i ranges over the whole population at time s , (and then s ranges from 0 to t). When a division occurs, produced by the cell i with age $a_i(Z_{s-}^{(k)})$, k newborn cells are created with age 0 at time s , that will have the same age $t - s$ at time t . We thus add to the system the term $k\delta_{t-s}$;
- removing the ages of the mother cells. This comes from the dying mother cell at time s and age $a_i(Z_{s-}^{(k)})$, according to the same division event as for the addition of newborn cells. This cell would have age $a_i(Z_{s-}^{(k)}) + t - s$ at time t , and therefore, we remove to the system the term $\delta_{a_i(Z_{s-}^{(k)})+t-s}$.

Whenever the integrator is a jump measure, we must be careful to consider integrands that are predictable in the sense of stochastic calculus, hence

the left limits in terms involving $a_i(Z_{s-})$. This is innocuous at the informal level we keep here, but becomes crucial whenever martingales properties are involved, that are essential to properly define existence and uniqueness of a measure solution $(Z_t^{(k)})_{t \geq 0}$ to (2.3).

Note that it is not completely obvious that a solution $(Z_t^{(k)})_{t \geq 0}$ to (2.3) exists, as well as its uniqueness. This is obtained by classical arguments and we refer to [41, 42] for a comprehensive treatment of the subject.

From the stochastic evolution (2.3) to a deterministic PDE

Consider the following renewal equation:

$$\begin{cases} \frac{\partial}{\partial t} n_k(t, a) + \frac{\partial}{\partial a} n_k(t, a) + B(a)n_k(t, a) = 0, \\ n_k(t, 0) = k \int_0^\infty B(a)n_k(t, a)da, \\ n_k(0, a) = n^{in}(a), \quad \int_0^\infty n^{in}(a)da = 1, \end{cases} \quad (2.4)$$

This is a classical model that goes back to McKendricks and von Foerster, see in particular the textbooks [46, 34]. If n^{in} and B are well-behaved there is existence and weak uniqueness of (2.4), see Prop. 3.3. Moreover, the solution $n_k(t, da) = n_k(t, a)da$ is absolutely continuous. Define for $t \geq 0$ the deterministic family of positive measures $(m_k(t))_{t \geq 0}$ via

$$\langle m_k(t, \cdot), \varphi \rangle = \int_0^\infty \varphi(a)m_k(t, da) = \mathbb{E}[\langle Z_t^{(k)}, \varphi \rangle],$$

with $m_k(0, da) = n^{in}(a)da$. The interpretation of m is the mean, or macroscopic state of the system. The link between the stochastic evolution (2.3) and the deterministic Fokker-Planck equation (2.4) is given by the following simple equivalence:

Proposition 2.2: *Assume that B is continuous and bounded and that the initial condition n^{in} is absolutely continuous, with a bounded continuous density. We then have $m_k = n_k$.*

These conditions are not minimal. We detail the essential steps of the proof of Proposition 2.2, since it illustrates in a relatively simple framework the interplay between deterministic and stochastic methods. The other equivalence results between random measure evolution equations and structured population equations stated in Section 2.3 are obtained in the same way.

Proof: *Step 1)* The action of time and age test functions (2.3). Let $\varphi_t(a) = \varphi(t, a)$ denote a test function (assumed to be smooth and compactly supported for safety). First, by definition of (2.3),

$$\begin{aligned} \langle Z_t^{(k)}, \varphi_t \rangle &= \langle \tau_t Z_0^{(k)}, \varphi_t \rangle + \int_0^t \sum_{i \leq \langle Z_{s-}^{(k)}, \mathbb{1} \rangle} \int_0^\infty \\ &\quad (k\varphi_t(t-s) - \varphi_t(a_i(Z_{s-}^{(k)}) + t-s)) \mathbb{1}_{\{\vartheta \leq B(a_i(Z_{s-}^{(k)}))\}} N_i(ds, d\vartheta). \end{aligned} \quad (2.5)$$

Next, for every $0 \leq s \leq t$, we have

$$\varphi_t(a+t-s) = \varphi_s(a) + \int_s^t \left(\frac{\partial}{\partial u} \varphi_u(a+s-u) + \frac{\partial}{\partial a} \varphi_u(a+s-u) \right) du.$$

Therefore, successively

$$\begin{aligned} \langle \tau_t Z_0^{(k)}, \varphi_t \rangle &= \sum_{i=1}^{\langle Z_0^{(k)}, \mathbb{1} \rangle} (\varphi_0(a_i(Z_0^{(k)}))) \\ &\quad + \int_0^t \left(\frac{\partial}{\partial s} \varphi_s(a_i(Z_0^{(k)}) + s) + \frac{\partial}{\partial a} \varphi_s(a_i(Z_0^{(k)}) + s) \right) ds, \\ \varphi_t(t-s) &= \varphi_s(0) + \int_s^t \left(\frac{\partial}{\partial u} \varphi_u(u-s) + \frac{\partial}{\partial a} \varphi_u(u-s) \right) du, \\ \varphi_t(a_i(Z_{s-}^{(k)}) + t-s) &= \varphi_s(a_i(Z_{s-}^{(k)})) + \\ &\quad \int_s^t \left(\frac{\partial}{\partial u} \varphi_u(a_i(Z_{s-}^{(k)}) + u-s) + \frac{\partial}{\partial a} \varphi_u(a_i(Z_{s-}^{(k)}) + u-s) \right) du. \end{aligned}$$

Plugging-in these three expansions in (2.5), and using the definition of $Z_s^{(k)}$ again, we obtain

$$\begin{aligned} \langle Z_t^{(k)}, \varphi_t \rangle &= \langle Z_0^{(k)}, \varphi_0 \rangle + \int_0^t \left\langle \frac{\partial}{\partial s} \varphi_s + \frac{\partial}{\partial a} \varphi_s, Z_s^{(k)} \right\rangle ds \\ &\quad + \int_0^t \sum_{i \leq \langle Z_{s-}^{(k)}, \mathbb{1} \rangle} \int_0^\infty (k\varphi_s(0) + \varphi_s(a_i(Z_{s-}^{(k)}))) \mathbb{1}_{\{\vartheta \leq B(a_i(Z_{s-}^{(k)}))\}} N_i(ds, d\vartheta). \end{aligned}$$

Step 2) A martingale-oriented representation of (2.3). We compensate the Poisson random measures $N_i(ds, d\vartheta)$ and define

$$\tilde{N}_i(ds, d\vartheta) = N(ds, d\vartheta) - ds \otimes d\vartheta.$$

For fixed φ , by construction, the random process

$$M_t(\varphi) = \int_0^t \sum_{i \leq \langle Z_{s-}^{(k)}, \mathbb{1} \rangle} \int_0^\infty (k\varphi_s(0) + \varphi_s(a_i(Z_{s-}^{(k)}))) \mathbb{1}_{\{\vartheta \leq B(a_i(Z_{s-}^{(k)}))\}} \tilde{N}_i(ds, d\vartheta)$$

is a centred martingale, and in particular $\mathbb{E}[M_t(\varphi)] = 0$. Noticing that

$$\begin{aligned} \sum_{i \leq \langle Z_{s-}^{(k)}, \mathbb{1} \rangle} \int_0^\infty (k\varphi_s(0) + \varphi_s(a_i(Z_{s-}^{(k)}))) \mathbb{1}_{\{\vartheta \leq B(a_i(Z_{s-}^{(k)}))\}} ds d\vartheta \\ = \langle Z_s^{(k)}, (k\varphi_s(0) - \varphi_s)B \rangle, \end{aligned}$$

we obtain from Step 1 the representation

$$\langle Z_t^{(k)}, \varphi_t \rangle = \langle Z_0^{(k)}, \varphi_0 \rangle + \int_0^t \langle \frac{\partial}{\partial s} \varphi_s + \frac{\partial}{\partial a} \varphi_s + (k\varphi_s(0) - \varphi_s)B, Z_s^{(k)} \rangle ds + M_t(\varphi).$$

Taking expectation and applying Fubini's theorem, we derive

$$\langle m_k(t, \cdot), \varphi_t \rangle = \langle m_k(0, \cdot), \varphi_0 \rangle + \int_0^t \langle \frac{\partial}{\partial s} \varphi_s + \frac{\partial}{\partial a} \varphi_s + (k\varphi_s(0) - \varphi_s)B, m_k(s, \cdot) \rangle ds. \quad (2.6)$$

Step 3: From (2.6) to (2.4). We finally prove that (2.6) and (2.4) are equivalent, along a classical line of arguments: we take for granted that $m_k(t, da) = m_k(t, a)da$ is absolutely continuous. This is a consequence of the smoothness of the initial condition and of B , see Prop. 3.3. We refer to [34] for transport equations or to [41] for a probabilist point of view. We evaluate its time derivative against a test function ϕ that depends on age only using (2.6). We obtain, for a nice enough ϕ so that we can interchange integral and derivative:

$$\frac{d}{dt} \int_0^\infty \phi(a) m_k(t, a) da = \int_0^\infty \left(\frac{\partial}{\partial a} \phi(a) + (k\phi(0) - \phi(a))B(a) \right) m_k(t, a) da.$$

Assume now that ϕ is compactly supported and smooth, and that moreover $\phi(0) = 0$. Integrating by part

$$\int_0^\infty \left(\frac{\partial}{\partial a} \phi(a) m_k(t, a) \right) da = - \int_0^\infty \phi(a) \frac{\partial}{\partial a} m_k(t, a) da.$$

We infer that for every such ϕ : $\frac{d}{dt} \langle m_k(t, \cdot), \phi \rangle = - \int_0^\infty \left(\frac{\partial}{\partial a} m_k(t, a) + B(a) m_k(t, a) \right) \phi(a) da$ and therefore

$$\frac{\partial}{\partial t} m_k(t, a) + \frac{\partial}{\partial a} m_k(t, a) + B(a) m(t, a) = 0 \quad da - \text{almost everywhere}$$

using one more time that $\phi(0) = 0$ to eliminate the term involving $k\phi(0)$. Now, consider an arbitrary test function ϕ vanishing at infinity: from the previous computation, we have

$$\begin{aligned} 0 &= \int_0^\infty \left(\frac{\partial}{\partial t} m_k(t, a) + \frac{\partial}{\partial a} m_k(t, a) \right) \phi(a) da \\ &= -\phi(0) m_k(t, 0) + k\phi(0) \int_0^\infty m_k(t, a) B(a) da \end{aligned}$$

and simplifying, we obtain the boundary condition $m_k(t, 0) = k \int_0^\infty B(a) m_k(t, a)$, as expected. This completes the proof. \square

2.3. Structured population equations

In the previous subsection, we have seen a rigorous derivation of the renewal equation from the stochastic differential equation. The same proof can be done in more intricate situations. For specific examples, we now give below the stochastic equation followed by the corresponding PDE, and the references for their rigorous derivation as well as some examples of possible generalisations.

Size-structured model: the growth-fragmentation process & equation

We structure the cell population according to the individual sizes $X_i(t)$ of each individual present at time t , encoded into the random point measure

$$Z_t^{(k)}(dx) = \sum_{i=1}^{\infty} \delta_{X_i(t)}(dx),$$

with values in $(0, \infty)$, the state space of sizes, and $k = 1$ or 2 refers to the number of cells that are kept into the system at division. The sum ranges from 1 to $\langle Z_t^{(k)}, \mathbb{1} \rangle$. Assuming that the sizes are ordered, the evaluation maps are defined as

$$x_i(Z_t^{(k)}) = x_i \left(\sum_{j=1}^{\infty} \delta_{X_j(t)}(dx) \right) = X_i(t).$$

In analogy to the age model described in the previous section, we have a stochastic evolution equation for the process $(Z_t^{(k)})_{t \geq 0}$:

$$Z_t^{(k)} = \exp(\kappa t) Z_0 + \int_0^t \sum_{i \leq \langle Z_{s-}^{(k)}, \mathbb{1} \rangle} \int_0^\infty (k \delta_{\frac{1}{2} x_i(Z_{s-}^{(k)}) \exp(\kappa(t-s))} - \delta_{x_i(Z_{s-}^{(k)}) \exp(\kappa(t-s))}) \mathbb{1}_{\{\vartheta \leq B(x_i(Z_{s-}^{(k)}))\}} N_i(ds, d\vartheta), \quad (2.7)$$

where, abusing notation slightly, for a random point measure $Z(dx) = \sum_{i=1}^\infty \delta_{z_i}(dx)$, and a real valued function ϕ , we set $\phi(Z)(dx) = \sum_{i=1}^\infty \delta_{\phi(z_i)}(dx)$, so that $\exp(\kappa t) Z_0 = \sum \delta_{X_i(0) e^{\kappa t}}$. Set, for (regular compactly supported) φ

$$\langle n_k(t, \cdot), \varphi \rangle = \mathbb{E} [\langle Z_t, \varphi \rangle],$$

We have (in a weak sense)

$$\frac{\partial}{\partial t} n_k(t, x) + \frac{\partial}{\partial x} (\kappa x n_k(t, x)) + B(x) n_k(t, x) = 2k B(2x) n_k(t, 2x). \quad (2.8)$$

The fact that the measure $\mathbb{E} [\langle Z_t, \cdot \rangle]$ solves (2.8) can be obtained along the same line of arguments as in Proposition 2.2. An alternative proof related on fragmentation processes, following the tagged fragment technique developed for instance in [43, 44], can be found in [37], for a more general model allowing variability in the growth rate κ .

Adder model: the incremental process \mathcal{E}^g structured equation

We structure the model in the pair of traits (x, z) where x denotes the size of a cell and z its size increment since its birth. We obtain a random measure

$$Z_t^i(dx, dz) = \sum_{i=1}^\infty \delta_{(X_i(t), Z_i(t))}(dx, dz),$$

where $(X_1(t), X_2(t) \dots)$ denotes the (ordered) size of each cell present in the system at time t (being born before t or course) and $Z_i(t)$ denotes the size increment of the cell with size X_i^b at birth. With these notation, the size $X_i(t)$ of a cell present in the system at time t is simply

$$X_i(t) = X_i^b + Z_i(t).$$

With the evaluation mappings

$$(x_i, z_i)(Z_t^i) = (x_i, z_i) \left(\sum_{j=1}^{\infty} \delta_{(X_j(t), Z_j(t))} (dx, dz) \right) = (X_i(t), Z_i(t)),$$

the stochastic evolution for the measure-valued process $(Z_t^i)_{t \geq 0}$ is given by

$$\begin{aligned} Z_t^i &= Z_0^i \exp(\kappa t) \\ &+ \int_0^t \sum_{i \leq \langle Z_{s-}^i, \mathbb{1} \rangle} \int_0^\infty \left(k \delta_{\left(\frac{1}{2} x_i(Z_{s-}^i) \exp(\kappa(t-s)), \frac{1}{2} x_i(Z_{s-}^i) (e^{\kappa(t-s)} - 1) \right)} \right. \\ &\quad \left. - \delta_{\left(x_i(Z_{s-}^i) e^{\kappa(t-s)}, x_i(Z_{s-}^i) e^{\kappa(t-s)} - (x_i(Z_{s-}^i) - z_i(Z_{s-}^i)) \right)} \right) \\ &\quad \times \mathbb{1}_{\{\vartheta \leq \kappa x_i(Z_{s-}^i) B(z_i(Z_{s-}^i))\}} N_i(ds, d\vartheta), \end{aligned} \quad (2.9)$$

where

$$Z_0^i \exp(\kappa t) = \sum_{i=1}^{\infty} \delta_{(x_i(Z_0^i) \exp(\kappa t), x_i(Z_0^i) \exp(\kappa t) - (x_i(Z_0^i) - z_i(Z_0^i)))} (dx, dz),$$

and similarly, set for (regular compactly supported) φ valued in $(0, \infty) \times (0, \infty)$

$$\langle n_k(t, \cdot, \cdot), \varphi \rangle := \mathbb{E} [\langle Z_t, \varphi \rangle],$$

We have (in a weak sense)

$$\frac{\partial}{\partial t} n_k + \frac{\partial}{\partial z} (\kappa x n_k) + \frac{\partial}{\partial x} (\kappa x n_k) = -\kappa x B(z) n_k(t, z, x), \quad (2.10)$$

$$\kappa x n_k(t, 0, x) = 4k\kappa x \int_0^\infty B(z) n_k(t, z, 2x) dz, \quad (2.11)$$

with $n_k(0, z, x) = n^{(0)}(z, x)$, $0 \leq z \leq x$.

Discussion on some generalisations

We can follow two variables, one behaving like a physiological age, *i.e.* reset at zero at each division, but which evolves with a non constant rate $\tau_z(z, x)$; the other behaving like a size, *i.e.* which is conserved by division through a fragmentation kernel $b(y, dx)$ such that $\int_0^y b(y, dx) = 1$, and growing at a rate $\tau_x(x, \kappa)$, with a parameter κ chosen at birth according to the rate κ' of the mother along a probability kernel $\theta(\kappa', d\kappa)$. We may assume that the division rate depends on size, growth rate and physiological age, and denote it $\beta(z, x, \kappa)$; we write it as a time instantaneous rate, contrarily to

the previous notations where B is an age or a size instantaneous rate, thus multiplied by the corresponding age or size growth rate. We expect the mean measure $n_k = \mathbb{E}[\langle Z_t, \cdot \rangle]$ of the corresponding population process to solve a PDE of the form

$$\frac{\partial}{\partial t} n_k + \frac{\partial}{\partial z} (\tau_z(z, x) n_k) + \frac{\partial}{\partial x} (\tau_x(x, \kappa) n_k) = -\beta(z, x, \kappa) n_k(t, z, x, \kappa), \quad (2.12)$$

$$\tau_x(0, \kappa) n_k(z, 0, \kappa) = 0, \quad \tau_z(0, \kappa) n_k(t, 0, x, \kappa) = \quad (2.13)$$

$$2k \int_0^\infty \int_0^\infty \int_0^\infty \theta(\kappa', \kappa) b(y, x) \beta(z, y, \kappa') n_k(t, z, y, \kappa') dz dy d\kappa'.$$

We recover the age model by taking $\beta(z, x, \kappa) = B(z)$, $\tau_z \equiv 1$, and integrating in size and growth rate; the size model with variable growth rate and unequal fragmentation by taking $\beta(z, x, \kappa) = \tau_x(x, \kappa) B(x)$ and integrating in z ; the increment model with variable growth rate by taking $\tau_z = \tau_x$, $\beta(z, x, \kappa) = \tau_x(x, \kappa) B(z)$. A detailed study lies beyond the level intended in these notes but the interest is to embed all the models considered here in a common framework.

3. Model analysis: long-time behaviour

Having built kinetic models leads naturally mathematicians towards the question of their long-time behaviour. In this matter, this is far from being a pure mathematical question: it reveals the cornerstone of our calibration strategy, developed in Section 4. It is however a whole field in itself: as in Section 2, we provide the main ingredients in the simplest case of the renewal equation and process - which already reveals not so simple when we study the stochastic population model - and review - not exhaustively - the extremely rich literature for more involved cases.

Importantly, we only consider here linear models, *i.e.* we neglect feedbacks or exchanges with the environment or between the cells; we only mention a few nonlinear results. When linear, the study of the asymptotic behaviour of the equations are closely related to the spectral analysis of the related semigroup operator, and leads to three main types of behaviours:

- convergence to a steady state (exponentially fast in case of a spectral gap), which happens for the conservative equations (case $k = 1$: ge-nealogical observation);

- steady exponential growth, *i.e.* there is a decoupling between an exponential growth at the rate of the dominant eigenvalue, called the *Malthusian parameter* or *fitness* of the population, and a steady distribution in the structuring variables. This happens in the case $k = 2$, where all the population is followed. As for the conservative case, an exponentially-fast trend to this steady behaviour is linked to a spectral gap.
- Other non physical behaviours, for instance spreading in the distributions, or yet trend to a permanently oscillating system, together with exponential growth in the case $k = 2$. This last case is a non-robust behaviour, linked to some degeneracy in the coefficients, so that the dissipation of entropy is not sufficient for a trend to a steady behaviour to emerge; it can also be seen as another type of convergence towards the dominant eigenvector, when this one becomes non unique. Whatsoever, this last behaviour, in the case of linear equations, is a mathematical curiosity rather than biologically informative. The interest of proving such non physical results consists in excluding some models or assumptions as non realistic if they lead to such non physical results.

These considerations drive our assumptions: they need to ensure the convergence of both the conservative ($k = 1$) and the nonconservative ($k = 2$) equations towards steady behaviours.

3.1. The renewal equation: a pedagogical example

This is historically the first structured-population model to be studied [45, 46]; another key reference is [26] around 1950 and later the celebrated textbook book by Harris [47]. There are strong links with the classical renewal theory of random walks in probability, that dates back to classics: W. Feller, J. Doob, A. Lotka [48, 49, 50]. A recent account of the link between fragmentation processes and renewal theory can be found in the textbook by J. Bertoin [43].

Let us denote the renewal equation in one of its simplest form:

$$\begin{cases} \frac{\partial}{\partial t} n(t, a) + \frac{\partial}{\partial a} n(t, a) = -B(a)n(t, a), \\ n(t, 0) = k \int_0^\infty B(a)n(t, a) da, \quad n(0, a) = n^0(a). \end{cases} \quad (3.1)$$

This equation has to be understood first in a weak sense, *i.e.* as an equivalent way to write (2.4)

Functional spaces through the lense of modelling

To give a rigorous meaning to this equation, either in a weak or strong formulation, one first needs to decide in which functional space - in the structuring variable (age here), then time - the solution n should be considered.

Closer to the stochastic process and to non-asymptotic or not-averaged populations are measure-valued solutions, see the recent and very pedagogical approach of P. Gabriel [51] for the case $k = 1$, or [52]: this allows one to consider measure-valued initial conditions for n^0 .

Convenient to handle the inverse problem or to use Fourier or Mellin transforms are L^2 -types spaces, see e.g. [12], but they lack physical interpretation. Assuming however that biological populations are expected to be in both L^1 and L^∞ , this is acceptable, for mathematical reasons, to choose such spaces.

Finally, weighted L^1 spaces have been widely used, for semi-group approaches [46] as well as for general relative entropy [34] or still others [53]. They have the advantage of immediate physical interpretation, since $\int n(t, a) da$ and $\int B(a)n(t, a) da$ represent respectively (the expectation of) the total number of individuals and the total number of dividing individuals at time t , $\int an(t, a) da$ the average age of individuals at time t , etc. Moreover, assuming $n(t, \cdot) \in L^1((0, \infty))$ means that the expectation of the stochastic measure has a density and, up to a renormalization if $k = 2$, is a probability density. At least for large times, we consider that this is relevant in a modelling perspective, and thus privilege this last family of functional spaces.

Let us briefly recall how the main results may be found using the entropy approach developed in [54], and discuss the links between the cases $k = 0$ and $k = 1$ - we refer to [34], chapter 2 for a complete presentation.

We assume

$$\begin{aligned} B &\in L_{loc}^\infty((0, \infty), [0, \infty)), \\ \int_0^\infty B(x) dx &= \infty, \quad \int_0^\infty xB(x)e^{-\int_0^x B(a) da} dx < \infty. \end{aligned} \tag{3.2}$$

These assumptions have a stochastic interpretation: if A is a random variable representing the age at division of a cell, the fact that $\int_0^\infty B(x) dx = \infty$ ensures that all cells divide. The probability density of A being the function $x \mapsto B(x)e^{-\int_0^x B(a) da}$, the last assumption means that $\mathbb{E}[A] < \infty$.

Eigenelements

As said in the introduction, the asymptotic behaviour is closely linked to the study of the spectrum of the linear operator under consideration: we may formally write

$$\frac{d}{dt}n(t, \cdot) = \mathcal{A}_k n(t, \cdot)$$

where \mathcal{A}_k is defined by (3.1). Eigenelements $(\lambda_k, N_k, \varphi_k)$ are solutions to the equations

$$\mathcal{A}_k N_k = \lambda_k N_k, \quad \mathcal{A}_k^* \varphi_k = \lambda_k \varphi_k,$$

where \mathcal{A}_k^* is the adjoint operator to \mathcal{A}_k , defined by the following adjoint equation

$$\mathcal{A}_k^* \varphi(a) := \frac{\partial}{\partial a} \varphi(a) - B(a) \varphi(a) + kB(a) \varphi(0).$$

Proposition 3.1: *Under Assumption (3.2), for $k = 1$ and $k = 2$, there exists a unique solution $(\lambda_k, N_k, \varphi_k)$ to the system*

$$\begin{cases} \lambda_k N_k(a) + \frac{\partial}{\partial a} N_k(a) + B(a) N_k(a) = 0, & \int_0^\infty N_k(a) da = 1, \\ N_k(0) = k \int_0^\infty B(a) N_k(a) da, \\ \lambda_k \varphi_k(a) - \frac{\partial}{\partial a} \varphi_k(a) + B(a) \varphi_k(a) = kB(a) \varphi_k(0), & \int_0^\infty N_k(a) \varphi_k(a) da = 1. \end{cases} \quad (3.3)$$

Moreover, we have $\lambda_1 = 0$, $\varphi_1 \equiv 1$, $\lambda_2 > 0$, $N_k, \varphi_2 > 0$, λ_2 is uniquely defined by the relation

$$1 = 2 \int_0^\infty B(a) e^{-\lambda_2 a - \int_0^a B(s) ds} da, \quad (3.4)$$

and $\varphi_2 \in L^\infty(0, \infty)$, $\varphi_2(0) > 0$ with the uniform bound

$$\|\varphi_2\|_{L^\infty} \leq 2\varphi_2(0) = 2 \frac{\int_0^\infty e^{-\lambda_2 a - \int_0^a B(s) ds} da}{\int_0^\infty s B(s) e^{-\lambda_2 s - \int_0^s B(\sigma) d\sigma} ds}.$$

Proof: The fact that $\varphi_1 \equiv 1$ can be seen directly from the fact that for $k = 1$ the equation is conservative. In the case of the renewal equation, contrarily to more involved cases where the study of existence and uniqueness

of eigenlements is a field in itself (see Section 3.3), we can immediately compute that solutions must satisfy

$$\begin{cases} N_k(a) = N_k(0)e^{-\lambda_k a - \int_0^a B(s)ds}, & N_k(0) = N_k(0)k \int_0^\infty B(a)e^{-\lambda_k a - \int_0^a B(s)ds} da, \\ \varphi_k(a) = \varphi_k(0) \left(1 - k \int_0^a B(s)e^{-\lambda_k - \int_0^s B(\sigma)d\sigma} ds\right) e^{\lambda_k a + \int_0^a B(s)ds} \\ \quad = k\varphi_k(0) \int_a^\infty B(s)e^{-\lambda_k(s-a) - \int_a^s B(\sigma)d\sigma} ds \end{cases} \quad (3.5)$$

From this relation and from Assumption (3.2), we deduce that $\lambda_1 = 0$ and obtain that λ_2 satisfies (3.4) from the boundary condition at $a = 0$. Since the right-hand side of (3.4) is a continuously decreasing function of λ_2 that equals 2 for $\lambda_2 = 0$ (thanks to the fact that $\int_0^\infty Bdx = \infty$) and vanishes for $\lambda \rightarrow \infty$, this defines a unique $\lambda_2 > 0$. The normalisation condition $\int_0^\infty N_k(a)da = 1$ ensures uniqueness of N_k (and the convergence of the integral $\int_0^\infty N_1(a)da = 1$ is guaranteed by the assumption $\int xB(x)e^{\int_0^x Bda} < \infty$); the normalisation condition $\int_0^\infty N_k(a)\varphi_k(a)da = 1$ ensures uniqueness of φ_k . The uniform bound for φ_2 is obtained by integrating by parts (3.5):

$$\varphi_2(a) = 2\varphi_2(0) \left(1 - \int_a^\infty \lambda_2 e^{-\lambda_2(s-a) - \int_a^s B(\sigma)d\sigma} ds\right) \leq 2\varphi_2(0),$$

and we compute

$$\begin{aligned} 1 &= \int_0^\infty N_2(a)da \implies N_2(0) = \left(\int_0^\infty e^{-\lambda_2 a - \int_0^a B(s)ds} da\right)^{-1}, \\ 1 &= \int_0^\infty N_2(a)\varphi_2(a)da = N_2(0)\varphi_2(0) \int_0^\infty \int_a^\infty B(s)e^{-\lambda_2 s - \int_0^s B(\sigma)d\sigma} ds da \\ &= N_2(a)\varphi_2(a) \int_0^\infty sB(s)e^{-\lambda_2 s - \int_0^s B(\sigma)d\sigma} ds \\ \implies \varphi_2(0) &= \frac{\int_0^\infty e^{-\lambda_2 a - \int_0^a B(s)ds} da}{\int_0^\infty sB(s)e^{-\lambda_2 s - \int_0^s B(\sigma)d\sigma} ds}. \quad \square \end{aligned}$$

Remark 3.2: We may find a solution for $k = 2$ under the relaxed assumption

$$B \in L_{loc}^\infty((0, \infty), [0, \infty)), \quad \int_0^\infty B(x)dx > \ln(2),$$

which is weaker than (3.2). This would however lead to $\lambda_1 < 0$ in the case where $\int_0^\infty Bdx < \infty$, so that the conservative equation would have no conservative eigenvector, *i.e.* no possible trend to a steady behaviour,

what should be excluded for modelling purpose. Similarly, if the assumption $\int xB(x)e^{-\int_0^x B da} dx < \infty$ is not fulfilled, we cannot normalise the eigenpair by $\int N_1\varphi_1 dx = 1$ because $\int N_1\varphi_1 dx = \infty$ in this case.

Existence of solutions

Many methods are available to prove existence and uniqueness of solutions in various spaces; we specially refer the interested reader to [46, 34] and for measure solutions to [51]. We only mention here an easy proof obtained by the Banach-Picard fixed point theorem and Duhamel's formula, inspired by [34], chapter 3, [55] Appendix B and [51] (solution for the dual equation). We take an L^1 space which is natural for solutions, namely $L^1((1+B(a))da)$, so that the assumptions on B are minimal.

Proposition 3.3: *For $B \in L_{loc}^\infty((0, \infty); (0, \infty))$ such that $\int_0^\infty B(a)da = \infty$, for $n^0 \in L^1((1+B(a))da)$, there exists a unique solution $n \in L_{loc}^\infty(0, \infty; L^1((1+B(a))da))$ to (3.1) and we have the comparison principle:*

$$\forall x, n_1^0(a) \leq n_2^0(a) \implies n_1(t, a) \leq n_2(t, a) \quad \forall t, a \geq 0.$$

Proof: Let $\lambda > 0$ a given constant. We look for solutions $\tilde{n}(t, a) = e^{-\lambda t}n(t, a)$ to the equation

$$\begin{cases} \frac{\partial}{\partial t}\tilde{n}(t, a) + \frac{\partial}{\partial a}\tilde{n}(t, a) + \lambda\tilde{n} = -B(a)\tilde{n}(t, a), \\ \tilde{n}(t, 0) = k \int_0^\infty B(a)\tilde{n}(t, a)da, \quad \tilde{n}(0, a) = n^0(a). \end{cases}$$

We define $\psi(t) = \tilde{n}(t, t+a)$ which is solution to

$$\psi'(t) + (B(t+a) + \lambda)\psi = 0, \quad \psi(0) = n^0(a),$$

and similarly $\tilde{\psi}(t) = \tilde{n}(t+a, t)$ is solution to

$$\tilde{\psi}' + (B(t) + \lambda)\tilde{\psi} = 0, \quad \tilde{\psi}(0) = \tilde{n}(a, 0) = k \int_0^\infty B(s)\tilde{n}(a, s)ds$$

so that we find the Duhamel's formula

$$\begin{aligned} \tilde{n}(t, a) &= n^0(a-t)e^{-\int_0^t B(s+a)ds - \lambda t} \mathbb{1}_{\{a \geq t\}} \\ &\quad + ke^{-\int_0^a B(\sigma)d\sigma - \lambda a} \int_0^\infty B(s)\tilde{n}(t-a, s)ds \mathbb{1}_{\{t \geq a\}}. \quad (3.6) \\ &:= \Gamma_{n^0}[\tilde{n}](t, a) \end{aligned}$$

We consider the mapping Γ_{n^0} taken on the weighted space $X = L^\infty(0, \infty; L^1((\frac{\lambda}{2k} + B(a)) da))$: we find, for any $t \geq 0$,

$$\begin{aligned} & \int_0^\infty \left| \left(\frac{\lambda}{2k} + B(a) \right) \Gamma[n_1 - n_2](t, a) \right| da \\ & \leq \int_0^\infty k \left(\frac{\lambda}{2k} + B(a) \right) e^{-\int_0^a B(\sigma) d\sigma - \lambda a} da \|n_1 - n_2\|_X \\ & \leq k \left(1 + \int_0^\infty \left(\frac{\lambda}{2k} - \lambda \right) e^{-\lambda a} da \right) \|n_1 - n_2\|_X \\ & \leq \frac{1}{2} \|n_1 - n_2\|_X. \end{aligned}$$

This proves that Γ is a strict contraction on X , hence applying the Banach-Picard fixed point theorem we find a unique fixed point, which is solution to (3.1). The comparison principle comes from the fact that if $n_0^1 \leq n_0^2$ then $\Gamma_{n_0^1}[n] \leq \Gamma_{n_0^2}[n]$; we can iterate each of the operators $\Gamma_{n_i^0}$ and at the limit we find $\tilde{n}_1 \leq \tilde{n}_2$, hence $n_1 \leq n_2$. \square

General relative entropy

A general fact shared by many linear population dynamics equations is a wide class of time-decreasing functionals, which may be used as a key ingredient to study the equation, in particular to prove long-time asymptotics [35] or uniqueness of eigensolutions [36]. We refer to [34] for a thorough presentation in many situations.

Lemma 3.4: *Let $H : [0, \infty) \rightarrow [0, \infty)$ a convex differentiable function, and n_1, n_2 two solutions of (3.1) in $L_{loc}^\infty([0, \infty); L^1((1 + B(a)) da))$ such that $n_2(t, x) > 0$ for all $t, x \geq 0$, and such that $\int \varphi_k(a) n_2(0, a) H\left(\frac{n_1(0, a)}{n_2(0, a)}\right) da < \infty$. We have the following inequality:*

$$\mathcal{H}(t) := \int \varphi_k(a) e^{-\lambda_k t} n_2(t, a) H\left(\frac{n_1(t, a)}{n_2(t, a)}\right) da \quad \implies \quad \frac{d}{dt} \mathcal{H}(t) \leq 0. \quad (3.7)$$

Proof: We compute, using the equations and integrating by parts:

$$\begin{aligned}
\frac{d}{dt} \mathcal{H}(t) &= \int_0^\infty e^{-\lambda_k t} \left\{ (-\lambda \varphi_k(a) n_2(t, a) + \varphi_k(a) \partial_t n_2(t, a)) H\left(\frac{n_1}{n_2}(t, a)\right) \right. \\
&\quad \left. + \varphi_k(a) \left(\partial_t n_1(t, a) - \frac{n_1}{n_2}(t, a) \partial_t n_2(t, a) \right) H'\left(\frac{n_1}{n_2}(t, a)\right) \right\} da \\
&= \int_0^\infty e^{-\lambda_k t} \left\{ (-\lambda \varphi_k(a) n_2(t, a) + \varphi_k(a) (-\partial_a n_2(t, a) - B(a) n_2(t, a))) H\left(\frac{n_1}{n_2}(t, a)\right) \right. \\
&\quad \left. + \varphi_k(a) \left(-\partial_a n_1 - B n_1 - \frac{n_1}{n_2} (-\partial_a n_2 - B n_2) \right) (t, a) H'\left(\frac{n_1}{n_2}(t, a)\right) \right\} da \\
&= \int_0^\infty e^{-\lambda_k t} (-\lambda \varphi_k n_2 + \partial_a \varphi_k n_2 - B \varphi_k n_2) H\left(\frac{n_1}{n_2}\right)(t, a) da \\
&\quad + \int_0^\infty e^{-\lambda_k t} \varphi_k(a) \left(\partial_a n_1(t, a) - \frac{n_1}{n_2}(t, a) \partial_a n_2(t, a) \right) H'\left(\frac{n_1}{n_2}(t, a)\right) da \\
&\quad + e^{-\lambda_k t} \varphi_k n_2 H\left(\frac{n_1}{n_2}\right)(t, 0) + \int_0^\infty e^{-\lambda_k t} \varphi_k(a) \left(-\partial_a n_1 + \frac{n_1}{n_2} \partial_a n_2 \right) H'\left(\frac{n_1}{n_2}\right)(t, a) da \\
&= e^{-\lambda_k t} \left\{ \int_0^\infty -k \varphi_k(0) B(a) n_2(t, a) H\left(\frac{n_1}{n_2}(t, a)\right) da \right. \\
&\quad \left. + k \varphi_k(0) H\left(\frac{n_1}{n_2}(t, 0)\right) \int_0^\infty B(a) n_2(t, a) da \right\} \\
&= k \varphi_k(0) e^{-\lambda_k t} \int_0^\infty B(a) n_2(t, a) \left\{ -H\left(\frac{n_1}{n_2}(t, a)\right) + H\left(\int_0^\infty B(s) \frac{n_1(t, s)}{n_2(t, 0)} ds\right) \right\} da \\
&\leq 0,
\end{aligned}$$

the last inequality following by Jensen's inequality applied to the convex function H applied to the function $f(a) = \frac{n_1}{n_2}(t, a)$, with respect to the probability measure $B(a) \frac{n_2(t, a)}{n_2(t, 0)} da$. \square

Remark 3.5: In full generality, we could replace $\varphi_k(x) e^{-\lambda_k t}$ by any solution of the adjoint equation of (3.1). We can also relax the assumption on H differentiable, by taking a regularising sequence, since at the limit the terms involving H' cancel each other. For $k = 1$, we have $\varphi_k e^{-\lambda_k t} \equiv 1$: the "general relative entropy" is a standard relative entropy between n_1 and n_2 .

Long-time behaviour

The long-time behaviour of the solution n may be obtained by several methods: the semi-group theory [46, 56], the use of a Laplace transform [57], the general relative entropy [34] extended recently to measure solutions [52], use of invariants [58], and very recently for measure-valued solutions Harris theorem and Doeblin's conditions [59, 60]. Whatever the method, the general fact is that under suitable assumptions, we have the convergence

$$n_k(t, a)e^{-\lambda_k t} \rightarrow N_k(a) \int_0^\infty n_k^0(a)\varphi_k(a)da$$

with λ_k and N_k defined in Proposition 3.1, and this convergence is exponentially fast in functional spaces where a spectral gap may be proved. More specifically, let us cite the following result, adapted from [55], theorem 3.8.

Theorem 3.6: (*From* [55]) *Assume that there exists $a_0 > 0$, $\underline{B} > 0$, $p > 0$ and $\ell \in (p/2, p]$ such that $\forall a \in [a_0 + \mathbb{N}p, a_0\ell + \mathbb{N}p]$, $B(a) \geq \underline{B}$. Then there exist $C > 0$, $\rho > 0$ (which can be explicitly computed) such that for any positive finite measure μ^0 , there exists a unique measure-valued solution μ_t to (3.1) in a weak sense, and the following inequality holds:*

$$\|e^{-\lambda t} \mu_t - \langle \mu^0, \varphi_k \rangle N_k\|_{TV} \leq C \|\mu^0\|_{TV} e^{-\rho t},$$

where $\|\cdot\|_{TV}$ denotes the total variation norm.

Note that the assumptions are more restrictive than for the existence or the eigenproblem results, and still more restrictive to prove an exponential rate of convergence. To give an elementary intuition of this convergence, let us look at the case $B > 0$ constant: then, Proposition 3.1 shows that $\lambda_k = (k-1)B$, $\varphi_k \equiv 1$, $N_k(a) = kB e^{-kBa}$ and a simple integration of the equation implies

$$\int_0^\infty n(t, a)da = e^{(k-1)Bt} \int_0^\infty n^0(a)da,$$

we now go back to the Duhamel formula (3.6) and find

$$\begin{aligned} n(t, a) &= n^0(a-t)e^{-\int_0^t B(s+a)ds} \mathbb{1}_{\{a \geq t\}} + ke^{-\int_0^a B(\sigma)d\sigma} \int_0^\infty B(s)n(t-a, s)ds \mathbb{1}_{\{t \geq a\}} \\ &= n^0(a-t)e^{-Bt} \mathbb{1}_{\{a \geq t\}} + N_k(a)e^{\lambda_k t} \mathbb{1}_{\{t \geq a\}} \int_0^\infty n^0(a)\varphi_k(a)da. \end{aligned}$$

The first term of the right-hand side vanishes exponentially fast at rate B , and the second term of the right-hand side is the expected limit.

3.2. The renewal process

Let us first discuss some heuristics for the convergence of empirical measures for further statistical applications. In order to extract information about $a \mapsto B(a)$, we consider the empirical distribution for a test function g defined by

$$\mathcal{E}^T(g) = |\mathcal{V}_T|^{-1} \sum_{u \in \mathcal{V}_T} g(\zeta_u^T),$$

where

$$\mathcal{V}_T = \{u \in \mathcal{U}, b_u \leq T, b_u + \zeta_u > T\}, \quad (3.8)$$

i.e. the population of cells that are alive at time T , and $\zeta_u^T = T - b_u$ is the value of the age trait at time T . We expect a law of large number as $T \rightarrow \infty$.

Heuristically, we postulate for large T the approximation

$$\mathcal{E}^T(g) \sim \frac{1}{\mathbb{E}[|\mathcal{V}_T|]} \mathbb{E} \left[\sum_{u \in \mathcal{V}_T} g(\zeta_u^T) \right].$$

Then, a classical result based on renewal theory (see Theorem 17.1 pp 142-143 of [47]) gives the estimate

$$\mathbb{E}[|\mathcal{V}_T|] \sim \kappa_B e^{\lambda_2 T},$$

where $\lambda_2 > 0$ is the Malthusian parameter of the model, defined as the unique solution to

$$\int_0^\infty B(x) e^{-\lambda_2 x - \int_0^x B(u) du} dx = \frac{1}{2},$$

as in (3.4), and $\kappa_B > 0$ is an explicitly computable constant. As for the numerator, call χ_t the size of a particle at time t along a branch of the tree picked at random. The process $(\chi_t)_{t \geq 0}$ is Markov process with values in $[0, \infty)$ with infinitesimal generator

$$\mathcal{A}g(x) = g'(x) + B(x)(g(0) - g(x)) \quad (3.9)$$

densely defined on bounded continuous functions. It is then relatively straightforward to obtain the identity

$$\mathbb{E} \left[\sum_{u \in \mathcal{V}_T} g(\zeta_u^T) \right] = \mathbb{E} [2^{N_T} g(\chi_T)], \quad (3.10)$$

where $N_t = \sum_{s \leq t} \mathbf{1}_{\{\chi_s - \chi_{s-} > 0\}}$ is the counting process associated to $(\chi_t)_{t \geq 0}$. Putting together $\mathbb{E} [|\mathcal{V}_T|] \sim \kappa_B e^{\lambda_2 T}$ and (3.10), we thus expect

$$\mathcal{E}^T(g) \sim \kappa_B^{-1} e^{-\lambda_2 T} \mathbb{E} [2^{N_T} g(\chi_T)],$$

and we anticipate that the term $e^{-\lambda_2 T}$ should somehow be compensated by the term 2^{N_T} within the expectation. To that end, following [61] (and also [32] when B is constant) one introduces an auxiliary “biased” Markov process $(\tilde{\chi}_t)_{t \geq 0}$, with generator $\mathcal{A}_{H_B} g(x) = \mathcal{A}g(x) = g'(x) + H_B(x)(g(0) - g(x))$ for a biasing rate $H_B(x)$ characterised by

$$f_2(x) = H_B(x) \exp\left(-\int_0^x H_B(y) dy\right),$$

with

$$f_2(x) = 2e^{-\lambda_2 x} f_1(x), \quad x \geq 0, \quad (3.11)$$

where

$$f_1(a) = B(a) \exp\left(-\int_0^a B(s) ds\right)$$

is the typical lifetime of a cell (without observation bias), or equivalently the density distribution of ζ_u , see (4.3) below. This choice (and actually this choice only) enables us to obtain

$$e^{-\lambda_2 T} \mathbb{E} [2^{N_T} g(\chi_T)] = 2^{-1} \mathbb{E} [g(\tilde{\chi}_T) B(\tilde{\chi}_T)^{-1} H_B(\tilde{\chi}_T)] \quad (3.12)$$

with $\tilde{\chi}_0 = 0$. Moreover $(\tilde{\chi}_t)_{t \geq 0}$ is geometrically ergodic, with invariant probability $c_B \exp(-\int_0^x H_B(y) dy) dx$. We further anticipate

$$\begin{aligned} \mathbb{E} [g(\tilde{\chi}_T) B(\tilde{\chi}_T)^{-1} H_B(\tilde{\chi}_T)] &\sim c_B \int_0^\infty g(x) B(x)^{-1} H_B(x) e^{-\int_0^x H_B(y) dy} dx \\ &= 2c_B \int_0^\infty g(x) e^{-\lambda_2 x} B(x)^{-1} f_1(x) dx \end{aligned}$$

assuming everything is well-defined, by (3.11). Finally, we have $\kappa_B^{-1} c_B = 2\lambda_2$ which enables us to conclude

$$\mathcal{E}^T(g) \rightarrow \mathcal{E}(g) := 2\lambda_2 \int_0^\infty g(x) e^{-\lambda_2 x} e^{-\int_0^x B(y) dy} dx \quad (3.13)$$

as $T \rightarrow \infty$. The convergence is in probability, with some explicit rate linked to λ_2 , as given below.

Definition 3.7: The family of (real-valued) random variables $(\Upsilon_T)_{T>0}$ is asymptotically bounded in probability if

$$\limsup_{T \rightarrow \infty} \mathbb{P}(|\Upsilon_T| \geq K) \rightarrow 0 \quad \text{as } K \rightarrow \infty.$$

In other words, the family of distributions of the random variables Υ_T is tight, or weakly relatively compact on a neighbourhood of $T = \infty$.

Proposition 3.8: Rate of convergence for particles living at time T (*Theorem 3 in [14]*) Assume $\lambda_2 \leq 2 \inf_x H_B(x)$. If B is differentiable and satisfies $B'(x) \leq B(x)^2$ and $0 < c \leq B(x) \leq 2c$ for every $x \geq 0$ and some $c > 0$, then

$$e^{\lambda_2 T/2} (\mathcal{E}^T(g) - \mathcal{E}(g))$$

is asymptotically bounded in probability.

3.3. The growth-fragmentation equation

When the structuring variable is the size, the so-called growth-fragmentation equation appears in many applications, from TCP-IP protocol to polymerization reactions. Let us write (2.8) here under a more general form, with a growth rate $\tau(x)$, a division rate $B(x) = \tau(x)B(x)$, an a fragmentation kernel $b(y, dx)$ representing the probability distribution (in dx) of the offspring of a dividing individual of size y :

$$\begin{cases} \frac{\partial}{\partial t} n_k(t, dx) + \frac{\partial}{\partial x} (\tau(x) n_k(t, dx)) = -B(x) \tau(x) n_k(t, dx) \\ \quad + k \int_{y=x}^{\infty} B(y) \tau(y) n(t, y) b(dy, x), \\ \tau(0) n_k(t, 0) = 0, \end{cases} \quad (3.14)$$

with two conditions ensuring conservation of mass through division and division into two (this second assumption is easily relaxed but this would be meaningless in our application context):

$$\int_0^y x b(y, dx) = \frac{y}{2}, \quad \int_0^y b(y, dx) = 1.$$

An important simplification often done is to restrict the equation to so-called *self-similar* division kernel b , meaning that the division place only depends on the ratio between the mother size and the daughter size: in such a case, we have

$$b(y, dx) := \frac{1}{y} b_0\left(\frac{dx}{y}\right), \quad \int_0^1 b_0(dz) = 1, \quad \int_0^1 z b_0(dz) = \frac{1}{2}, \quad (3.15)$$

and modelling considerations also lead to $b(y, dx) = b(y, y - dx)$, leading to b_0 symmetric in $1/2$ (in a still more general way, we may consider a stochastic number of children, see [43]). In the study of the equation, the moments

play a very important role, and the moments of order zero and one have a physical interpretation: integrating the equation, we obtain - formally at this stage

$$\frac{d}{dt} \int n_k(t, x) dx = (k-1) \int \tau(x) B(x) n_k(t, x) dx,$$

which means that for $k = 1$ the number of individuals is constant - the equation is conservative - whereas for $\varepsilon = 2$ it grows due to the division process. Integrating the equation against the weight x , we have

$$\frac{d}{dt} \int x n_k(t, x) dx = \left(\frac{k}{2} - 1\right) \int B(x) \tau(x) n_k(t, x) dx + \int \tau(x) n_k(t, x) dx,$$

which is easily interpreted: for $k = 1$ the mass increases with growth but decreases with division, whereas for $k = 2$ it only increases with growth. More generally, moments of order p show a balance between growth and division:

$$\frac{d}{dt} \int_0^\infty x^p n dx = \int_0^\infty \left(p - B(x)x \left(1 - k \int_0^x \frac{y^p}{x^p} b(x, dy) \right) \right) x^{p-1} \tau(x) n dx.$$

This balance between growth and division leads to the main asymptotic behaviour to be expected: the convergence to a steady size-distribution profile, with exponential growth in time for the population case $k = 2$, at an exponential rate of convergence if a spectral gap is proved. This study begins in the 1980's with the work by Diekmann, Heijmans, Thieme and Gyllenberg and Webb [62, 63], based on the theory of semigroups, and generally carried out under the assumption of a compact support for the size so that general theorems may apply in a more direct way. This has been then generalised by several authors, see [56, 55]. Explicit solutions, for power law rates and specific fragmentation kernels have also been studied [64, 65, 66].

Eigenelements

The eigenvalue problem and its adjoint are as follows:

$$\begin{cases} \frac{\partial}{\partial x} ((\tau N_k)(x)) + \lambda_k N_k(x) = -(\tau B N_k)(x) + k \int_x^\infty (\tau B N_k)(y) b(y, x) dy, \\ \tau N_k(x=0) = 0, \quad N_k(x) \geq 0, \quad \int_0^\infty N_k(x) dx = 1, \\ -\tau(x) \frac{\partial}{\partial x} (\varphi_k(x)) + \lambda_k \varphi_k(x) = B(x) \tau(x) (-\varphi_k(x) + k \int_0^x b(x, y) \varphi_k(y) dy), \\ \varphi_k(x) \geq 0, \quad \int_0^\infty \varphi_k(x) N_k(x) dx = 1. \end{cases} \quad (3.16)$$

These equations are meant in a weak sense, *i.e.* we look for $N_k \in L^1((0, \infty), dx)$ such that $\forall \phi \in \mathcal{C}_c^\infty([0, \infty))$ we have

$$-\int_0^\infty \tau N_k \partial_x \phi dx + \lambda \int_0^\infty \phi dx = \int_0^\infty B \tau N_k \left(k \int_0^x \phi(y) b(x, dy) - \phi(x) \right) dx,$$

and $\varphi \in W_{loc}^{1,\infty}$ is solution almost everywhere. For existence and uniqueness of eigenelements, the following assumptions are among the most general ones - except the fact that rates are at most polynomially growing, which is relaxed in Theorem 3.11 below, but which was useful in the proof of [36] based on moment estimates:

$$\text{Supp}(b(y, \cdot)) \subset [0, y], \quad \int_0^y b(y, dx) = 1,$$

$$\int_0^y x b(y, dx) = \frac{y}{2}, \quad \int_0^y \frac{x^2}{y^2} b(y, dx) \leq c < \frac{1}{2},$$

$$\tau, B \in \mathcal{P} := \left\{ f \geq 0 : \exists \mu, \nu \geq 0, \limsup_{x \rightarrow \infty} x^{-\mu} f(x) < \infty, \liminf_{x \rightarrow \infty} x^\nu f(x) > 0 \right\},$$

$$\tau B \in L_{loc}^1((0, \infty)), \quad \exists \alpha_0 \geq 0, \quad \tau \in L_{loc}^\infty([0, \infty), x^{\alpha_0} dx),$$

$$\forall K \text{ compact on } (0, \infty), \quad \exists m_K > 0, \quad \tau(x) \geq m_K \text{ a.e. } x \in K,$$

$$\exists B_0 \geq 0, C > 0, \gamma \geq 0, \text{Supp}(B) = [b, \infty), \int_0^x b(y, dz) \leq \min\left(1, C\left(\frac{x}{y}\right)^\gamma\right),$$

$$B, \frac{x^\gamma}{\tau} \in L_0^1 := L_{loc}^1([0, \cdot)), \quad \lim_{x \rightarrow \infty} xB = \infty.$$

(3.17)

Theorem 3.9: (*From* [36]) *Under the balance assumptions (3.17) on τ , B and b , there exists a unique triplet $(\lambda_k, N_k, \varphi_k)$ with $\lambda_2 > 0$, $\lambda_1 = 0$, $\varphi_1 \equiv 1$ solution of the eigenproblem (3.16) and*

$$x^\alpha \tau N_k \in L^p(\mathbb{R}^+), \quad \forall \alpha \geq -\gamma, \quad \forall p \in [1, \infty], \quad x^\alpha \tau N_k \in W^{1,1}(\mathbb{R}^+),$$

$$\exists p > 0 \text{ s.t. } \frac{\varphi_2}{1+x^p} \in L^\infty(\mathbb{R}^+), \quad \tau \frac{\partial}{\partial x} \varphi_2 \in L_{loc}^\infty(\mathbb{R}^+).$$

We notice that the assumptions on B at ∞ are very similar to the ones for the renewal equation. If $B(x) = x^\gamma$, the assumptions on B are satisfied for $1 + \gamma > 0$, see [67]. The proof is based on standard theorems for regularized equations (Krein-Rutman or Perron-Frobenius), the compactness obtained by successive moments estimates, and uniqueness by using general relative entropy inequalities.

Finally, a quick computation shows that in the case of exponential growth $\tau(x) \equiv x$ and of division into two equally-sized daughters $b(y, x) = \delta_{x=y/2}$, we have $\varphi_2(x) \equiv Cx$ with $C > 0$ a normalisation constant, and $N_1(x) = C'xN_2(x)$ with $C' > 0$ another normalisation constant.

General Relative Entropy

Lemma 3.10: (General Relative Entropy Inequality - [35], Theorem 2.1) *Let n_1, n_2 be two solutions of (3.14), with $n_2(t, x) > 0$ for all time and size, $H : \mathbb{R} \rightarrow [0, \infty)$ positive, differentiable and convex, and $\int_0^\infty \varphi(x)n_2(0, x)H\left(\frac{n_1}{n_2}(0, x)\right) dx < \infty$. Then we have*

$$\mathcal{H}(t) := \int_0^\infty \varphi(x)e^{-\lambda t}n_2(t, x)H\left(\frac{n_1}{n_2}(t, x)\right) dx, \quad \frac{d\mathcal{H}}{dt} = -D^H[n_1, n_2] \leq 0,$$

with

$$D^H[n_1, n_2](t) = \int_0^\infty \int_0^\infty k\varphi(x)e^{-\lambda t}n_2(t, y)\tau(y)B(y)b(y, x)$$

$$\left\{ H\left(\frac{n_1}{n_2}(t, y)\right) - H\left(\frac{n_1}{n_2}(t, x)\right) - H'\left(\frac{n_1}{n_2}(t, x)\right) \left\{ \frac{n_1}{n_2}(t, y) - \frac{n_1}{n_2}(t, x) \right\} \right\} dx dy.$$

We let the reader check directly this computation or refer to [68] or [34]. We also observe that the entropy for the renewal equation may be viewed as a specific case of this inequality: it suffices to take $b(y, x) = \delta_{x=0}$ and $\tau(x) = 1$. As for the renewal equation, it is possible to prove long-term convergence by means of this entropy inequality [34, 68], and exponential rate of convergence through entropy-entropy dissipation inequalities [69], *i.e.* if we can bound $-D^H$ by a quantity depending on \mathcal{H} .

Long time asymptotics: the central case of asynchronous exponential growth

Many methods have been developed to study the long time asymptotics of growth-fragmentation equations, from semi-group theory, general relative entropy, to methods inspired by stochastic processes such as several very recent studies [70, 71]. Let us cite here a recent result, carried out only for the two extreme cases of uniform (*i.e.* $b_0 = 2\mathbb{1}_{[0,1]}$) or equal mitosis (*i.e.* $b_0 = 2\delta_{1/2}$) fragmentation kernels, but relatively general for the assumption on the fragmentation rate, which may grow faster than polynomially.

Assumption 1: (**Assumptions for a spectral gap, see [71]**)

- $b(y, x) = \frac{2}{y} \mathbb{1}_{\{x \leq y\}}$ or $b(y, x) = 2\delta_{x=\frac{y}{2}}$.
- τ is locally Lipschitz, $g(x) = O(x)$ around ∞ , $g(x) = O(x^{-\xi})$ around 0 with $\xi \geq 0$,
- $B : (0, \infty) \rightarrow [0, \infty)$ is continuous,
- $\int_0 B dx < \infty$, $\lim_{x \rightarrow 0} xB(x) = 0$, $\lim_{x \rightarrow \infty} xB(x) = \infty$.
- If $b(y, x) = 2\delta_{x=\frac{y}{2}}$, the growth rate τ must moreover satisfy
 - $\omega g(x) < g(\omega x)$ for all $x > 0$ and $0 < \omega < 1$,
 - $H(z) := \int_0^z \tau^{-1}(z) dz < \infty$ for all $z > 0$,
 - $\lim_{z \rightarrow \infty} H^{-1}(z+r)/H^{-1}(z) = 1$.

Restricted to $\tau(x) = x^\nu$, we see that the assumptions imply $\nu \leq 1$ for the uniform kernel, $\nu < 1$ for the equal mitosis kernel, and allow any growth for B at infinity: compared to the assumptions for the existence of eigenelements, the main restriction, apart from the specific shapes of the fragmentation kernel, is that we cannot consider superlinear growth rates, since then the cell sizes may explode in finite time.

Theorem 3.11: (*Theorem 1.3 from [71]*) Under Assumptions 1, there exists a unique eigentriplet $(\lambda_2, N_2, \varphi_2)$ solution to (3.16). Let us denote, for $k \leq 0$ and $K > 1$, the following weighted total variation norm

$$\|\mu\|_{k,K} := \int_0^\infty (x^k + x^K) |\mu|(dx).$$

Then for n_0 a nonnegative finite measure satisfying $\|n_0\|_{k,K} < \infty$, there exists a unique measure-valued solution n_2 to (3.14) and it satisfies, for some $C > 0$ and $\rho > 0$,

$$\|e^{-\lambda_2 t} n_2(t, \cdot) - \langle \varphi_2, n_0 \rangle N_2\|_{k,K} \leq C e^{-\rho t} \|n_0 - \langle \varphi_2, n_0 \rangle N_2\|_{k,K},$$

with the following possible choices for k and K :

1. if $\int_0 \tau(x)^{-1} dx < \infty$, take $k = 0$ and any $K > 1 + \xi$,
2. if $\int_0 \tau(x)^{-1} dx = \infty$, take any $k \in (-1, 1)$ and $K > 1 + \xi$,
3. if $\tau(x) = x$, take any $k \in (-1, 1)$ and $K > 1$.

The assumptions on the state space where the convergence holds are crucial to obtain the exponential speed of convergence, which is linked to a spectral gap. Specifically, P. Michel, S. Mischler and B. Perthame proved convergence - without speed - in the weighted space $L^1(\varphi_2 dx)$ [35], which is the

most natural space to prove convergence results through the general relative entropy inequality; but under the assumption of bounded fragmentation rates, E. Bernard and P. Gabriel proved that there exists no spectral gap in this space: the convergence may hold arbitrarily slowly for well-chosen initial conditions, see Theorems 1.2 and 4.1 in [72]. Among other important results that we cannot review in detail here, let us cite fine estimates on the eigenvector and adjoint eigenvector [69, 73], semigroup approaches [56], probabilistic approaches [74, 75].

Long time asymptotics: other cases

When the balance assumptions between growth and division around zero and around infinity fail to be satisfied, other types of asymptotic behaviour may happen, leading to mass escape towards zero (dust formation or shattering) or infinity (gelation). Let us focus on the case of exponential growth $\tau(x) = x$, interesting in several ways: as already said, it is the idealised growth rate for many unicellular organisms, like bacteria; it is also the limit case before characteristic curves grow to infinity in finite time; last but not least, it appears by a change of variables when studying the asymptotic trend to a self-similar profile for the pure fragmentation equation, see [13] Theorem 3.2. Assuming a power law for the division rate $B(x) = x^\gamma$, we can classify the anomalous asymptotic behaviours according to the value of γ .

- $\gamma < -1$: in such a case, there is a loss of mass by dust formation in finite time called *shattering* [44, 76, 77, 78, 79, 80], non-uniqueness of solutions [81, 82].
- $\gamma = -1$: this is a case where the *time-dependent* division rate $\beta(x) = B(x)\tau(x)$ is constant. It is a limit case, where there is neither loss of mass in finite time nor convergence to a steady profile and exponential growth, since each moment of the equation grows or decays exponentially with a specific rate, see [83]. This is interesting from a modelling perspective because it explains the fact that a model with both exponential growth in size and size-independent division (for instance an age-structured division rate for exponentially growing cells) is irrelevant, leading to a non realistic exponential behaviour since no steady profile in size may be obtained [19]. Generalisations of this limit case to $\tau(x) = x^{1+\gamma}$ and $B(x)\tau(x) = x^\gamma$ with $\gamma > 0$, leading to blow-up in finite time, has been done by M. Escobedo [64, 84] and J. Bertoin and A. Watson for the corresponding stochastic processes [85].

- $\gamma > -1$: in general, convergence theorems such as Theorem 3.11 are valid, however for very specific division kernel such as the idealised equal mitosis case, the solution may converge to a cyclic behaviour. In such a case, we still have a general relative entropy inequality given by Lemma 3.10, but a simple computation shows that the entropy dissipation D^H vanishes not only for $\frac{n_1}{n_2}$ constant, but also for any ratio satisfying

$$\frac{n_1(x)}{n_2(x)} = \frac{n_1(2x)}{n_2(2x)},$$

which is a kind of periodicity condition. The best intuition on what happens here comes from the underlying stochastic branching tree: all descendants of a given cell of size x_0 at time 0 live on the countable set of curves $x_0 e^{t2^{-n}}$, due to the very specific relation between growth and division, whereas for other growth or division the times of division account, leading to a kind of dissipativity. This case has been studied by semigroup theory for compact support in size by G. Greiner and R. Nagel [86], and extended and revisited in [87] where the following explicit asymptotic result has been proved - see also [88] for extension to measure solutions.

Theorem 3.12: (*Theorem 2.3. in [87]*) Let $\tau > 0$ and define $\tau(x) = x$, $b(y, x) = 2\delta_{x=\frac{y}{2}}$, and B such that

$$\left\{ \begin{array}{l} B : (0, \infty) \rightarrow (0, \infty) \text{ is measurable, } B \in L^1_{loc}([0, \infty)), \\ \exists \gamma_0, \gamma_1, K_0, K_1, x_0 > 0, \quad K_0 x^{\gamma_0} \leq xB(x \geq x_0) \leq K_1 x^{\gamma_1}. \end{array} \right. \quad (3.18)$$

Theorem 3.9 holds, but there also exists a countable set of nonpositive dominant eigentriplets defined, for $m \in \mathbb{Z}$, by

$$\lambda_k^m = (k-1) + \frac{2im\pi}{\ln 2}, \quad N_k^m(x) = x^{-\frac{2im\pi}{\ln 2}} N_k^m(x), \quad \varphi_k^m(x) = c_m x^{k-1 + \frac{2im\pi}{\ln 2}},$$

with c_m normalisation constants. All the quantities $\langle n_k(t, \cdot), \varphi_k^m e^{-\lambda_k^m t} \rangle$ are then conserved, and for any $n_0 \in L^2([0, \infty), x^{k-1}/N_k^0(x)dx)$, the unique solution $n_k(t, x) \in C([0, \infty), L^2([0, \infty), x^{k-1}/N_k^0(x)dx))$ to (3.14) satisfies

$$\int_0^\infty \left| n_k(t, x) e^{-\kappa(k-1)t} - \sum_{m=-\infty}^\infty \langle n_0, \varphi_k^m \rangle N_k^m(x) e^{\frac{2im\pi}{\ln 2} t} \right|^2 \frac{x dx}{N_k^0(x)} \xrightarrow{t \rightarrow \infty} 0.$$

A numerical scheme needs to be non-dissipative to capture the oscillations, for instance by splitting transport and fragmentation and by using a geometric grid, see Section 3 in [87]; another way would be to use a splitting particle method [89].

3.4. Structured population equations and processes

For more general models and methods, several excellent books [46, 34, 90] have been written together with an extensive literature, mainly for linear but also for nonlinear [54, 91] cases, from a PDE or a stochastic point of view. Let us mention here only the expected asymptotic behaviour, given by the eigenvector(s) linked to the dominant eigenvalue(s), for the models cited in Section 2.3.

The incremental/adder model

The eigenvalue problem linked to the system (2.10)(2.11) may be written as follows:

$$\begin{cases} \lambda_k N_k + \frac{\partial}{\partial z}(\kappa x N_k) + \frac{\partial}{\partial x}(\kappa x N_k) = -\kappa x B(z) N_k(z, x), \\ \kappa x N_k(0, x) = 4k\kappa x \int_0^\infty B(z) N_k(z, 2x) dz, \end{cases} \quad (3.19)$$

with $\lambda_1 = 0$ as usual, and $\lambda_2 = \kappa$ as for the growth-fragmentation equation, due to the linear growth rate. Existence and uniqueness of a dominant positive eigenvalue and eigenvector has been recently studied in [92], for more general fragmentation kernels than just the diagonal kernel. Note also that in this specific case, we also have a countable set of dominant (not positive) eigenvalues, so that an equivalent of Theorem 3.12 may be obtained.

Generalisations

Several types of generalisations have been studied, for instance with varying growth rates [37], or with a maturity variable added to the renewal equation [54], size and age structured models [93, 94] etc. Let us only write here the eigenvalue problem related to (2.12)(2.13) - whose study once more lies

beyond the scope of this chapter:

$$\lambda_k N_k + \frac{\partial}{\partial z} (\tau_z(z, x) N_k) + \frac{\partial}{\partial x} (\tau_x(x, \kappa) N_k) = -\beta(z, x, \kappa) N_k(z, x, \kappa), \quad (3.20)$$

$$\begin{aligned} \tau_x N_k(z, 0, \kappa) &= 0, \quad N_k \geq 0, \quad \iiint N_k dz dx d\kappa = 1, \\ \tau_z(x, \kappa) N_k(0, x, \kappa) &= \\ 2k \int_0^\infty \int_0^\infty \int_0^\infty &\theta(\kappa', \kappa) b(y, x) \beta(z, y, \kappa) N_k(z, y, \kappa') dz dy d\kappa'. \end{aligned} \quad (3.21)$$

4. Model calibration: statistical estimation of the division rate

In Section 1.3, we have noticed that, contrarily to the growth rate or even to the division kernel, the division rate cannot be inferred from direct measurements, even from individual dynamics data. We thus face a typical inverse problem: How to estimate the division rate B from data on a population, which follows - we assume - the dynamics given by one of the structured population model described above?

A first and major idea [12] consists in taking advantage of the asymptotic analysis carried out in Section 3: we consider that at any time of the experiment, the population has already reached its steady asymptotic regime, *i.e.* for the observation scheme k that the population is aligned along the dominant eigenvector N_k of the model under consideration: age, size, increment, or more general model. This is well justified by the theoretical analysis above: the trend being exponentially fast under fairly general assumptions, the not-asymptotic regime concerns in most experimental cases only a negligible part of the data collected.

We recall (see Section 1.3) that there are two types of datasets, each being related to a different inverse problem:

- **Individual dynamics data collection:** following the trajectory of each individual allows us to measure the dividing and newborn cells. Intuitively, one feels that this allows a relatively direct estimation of the division rate. This type of data may concern genealogical (through *e.g.* microfluidic device) as well as population (microcolony growth) observation. A difficulty in the population dynamics observation is the selection bias [14].
- **Population point data:** we can observe, at given timepoints, samples of some structuring variables such as size (or age, fluorescent label [95] or

whatsoever), which are then related to the empirical distribution (2.2), itself related to $f_t(\cdot) = \frac{n_k(t, \cdot)}{\int n_k(t, \cdot) d}$ thanks to a representation like in Proposition 2.2. We may moreover assume an approximation of the form $f_t \approx N_k$ by the use of a time-asymptotic result such as Theorems 3.6 or 3.11. Alternatively, we can keep up with a stochastic approach, linking directly the stochastic measure to its limit through probabilistic results such as [37, 14, 75]. We then address the inverse problem consisting in estimating B from measurements of N_k ; one feels immediately that such an approach requires more analysis and, since the available information is less rich, that the inverse problem is more ill-posed.

Note that even in the case of individual dynamics collection, it may be more interesting to use the second approach: if the data are more numerous or less noisy, this may compensate the fact that the information they contain is poorer. In our example of *E. coli*, both approaches are possible, which allows to compare their accuracy in practice.

4.1. Estimating an age-dependent division rate

As for the previous sections 2 and 3.1, the age-structured model is somehow the simplest model along our line of models for which explicit computations can be conducted. We review here the different types of inverse problems we have to solve, depending on the type of data available; we will find all the same problems for the other models.

4.1.1. Individual dynamics data

Individual dynamics data, stochastic viewpoint. Let us assume that we have data such as shown in Figures 1 or 2: at short time intervals, we observe the age of cells, so that we observe

$$\{\zeta_u, u \in \mathcal{U}_k\},$$

for some subtree $\mathcal{U}_k \subset \mathcal{U}$, with \mathcal{U} being defined in (2.1). For the genealogical observation ($k = 1$), we define

$$\mathcal{U}_1 = \{u_\ell \in \{0, 1\}^\ell, u_{\ell+1} = (u_\ell, u^+), 0 \leq \ell \leq n, u^+ \in \{0, 1\}\}, \quad (4.1)$$

with $u^+ \in \{0, 1\}$ chosen uniformly at random, so that $u_{\ell+1}$ is offspring of u_ℓ , and n is a fixed number given by the experimentalist. In practice, we gather several such trees. For the population observation ($k = 2$), the trees

are defined by a final time $T > 0$ fixed by the experimentalist, so that we observe

$$\mathcal{U}_2 = \{u \in \mathcal{U}, b_u + \zeta_u \leq T\}, \quad (4.2)$$

where b_u is the birth time of the cell: we observe all the lifetimes of cells which have divided before T . We see that the number of cells is stochastic for this second case, and there is a selection bias: we will observe more descendants of cells which have divided quickly, see Section 3.

Individual dynamics data, stochastic viewpoint, genealogical observation. This case is relatively straightforward: as already observed, since

$$\mathbb{P}(\zeta_u \in [a, a + da] | \zeta_u \geq a) = B(a)da,$$

we obtain that the probability distribution of a lifetime ζ_u is given by

$$\mathbb{P}(\zeta_u \in da) = f_1(a)da = B(a) \exp\left(-\int_0^a B(s)ds\right)da. \quad (4.3)$$

In the case of a genealogical observation, the subtree is deterministic: there is no selection bias and the lifetime of each cell is independent from the others: we observe a sample of n cells having divided at ages which are the realizations of $\{\zeta_u, u \in \mathcal{U}_1\}$, as independent random variables with common density f . Moreover, as soon as $\int^\infty B = \infty$, we have the survival analysis representation

$$B(a) = \frac{f_1(a)}{\int_a^\infty f_1(s)ds} = \frac{f_1(a)}{S_1(a)}, \quad (4.4)$$

where S_1 is the survival function, as a simple inversion of the formula (4.3) given above. In other application contexts, B is called a hazard function. In this simple formula, we notice here three important facts, that will be found throughout our study:

- estimating B has the same complexity as estimating the density f_1 . This stems from the fact that the survival function $S_1(a)$ can be estimated at rate \sqrt{n} by its empirical counterpart, hence only the numerator in the right-hand side of (4.4) is a genuine nonparametric estimation problem.
- The estimation of $B(a)$ becomes harder as a increases, since $S(a)$ vanishes when a tends to infinity.
- We can also interpret our observations directly on the eigenvector equation N_1 : the proportion of dividing cells being $B(a)N_1(a)$, we find B by

writing simply

$$B(a) = \frac{B(a)N_1(a)}{N_1(a)},$$

and using the equation again we find that $N_1(a) = Ce^{-\int_0^a B(s)ds} = CS_1(a)$, with $C > 0$ a normalisation constant, so that we are back to (4.4).

We make the first point rigorous by recalling a standard statistical estimation result. Let $K : [0, \infty) \rightarrow \mathbb{R}$ denote a well-located kernel of order $\ell \geq 0$, namely

$$K \in \mathcal{C}_c^0(\mathbb{R}), \quad \int_0^\infty a^k K(a) da = \mathbb{1}_{\{k=0\}} \quad \text{for } k = 0, \dots, \ell. \quad (4.5)$$

The existence of such an oscillating kernel for arbitrary ℓ is standard, see *e.g.* the textbook [96]. For $h > 0$ the bandwidth, define $K_h(a) = h^{-1}K(h^{-1}a)$ and

$$\widehat{B}_{n,h}(a) = \frac{\sum_{u \in \mathcal{U}_1} K_h(a - \zeta_u)}{\sum_{u \in \mathcal{U}_1} \mathbb{1}_{\{\zeta_u \geq a\}}}, \quad (4.6)$$

(and set 0 if none of the ζ_u are above a .) The *bias* of f_1 at a relative to the approximation kernel K is defined as

$$\mathfrak{b}_h(f_1)(a) = \left| \int_{[0,\infty)} f_1(a') K_h(a - a') da' - f_1(a) \right|.$$

Proposition 4.1: *We have*

$$\begin{aligned} & \mathbb{E} \left[\left| |\mathcal{U}_1|^{-1} \sum_{u \in \mathcal{U}_1} K_h(a - \zeta_u) - f_1(a) \right|^2 \right] \\ & \leq \mathfrak{b}_h(f_1)(a)^2 + (nh)^{-1} \sup_{a-a' \in \text{Supp}(K)} B(a') \int_{[0,\infty)} K(a')^2 da' \end{aligned} \quad (4.7)$$

and

$$\mathbb{E} \left[\left| |\mathcal{U}_1|^{-1} \sum_{u \in \mathcal{U}_1} \mathbb{1}_{\{\zeta_u \geq a\}} - S_1(a) \right|^2 \right] \leq \frac{1}{4} n^{-1}. \quad (4.8)$$

Proof: The first part is obtained by noticing that $\int_{[0,\infty)} f_1(a') K_h(a - a') da' = \mathbb{E}[K_h(a - \zeta_u)]$, and using that the variables $K_h(a - \zeta_u) - \mathbb{E}[K_h(a - \zeta_u)]$ are independent and identically distributed, with common variance bounded above by $h^{-1} \int_{[0,\infty)} K_h(a - a')^2 f_1(a') da' \leq \sup_{a-a' \in \text{Supp}(K)} B(a') \int_{[0,\infty)} K(a')^2 da'$. The result is simply a combination

of this observation and the fact that the variance of the sum of independent random variables is the sum of its variances. The second part easily follows, noticing now that $\mathbb{1}_{\{\zeta_u \geq a\}}$ is a Bernoulli random variable with expectation $S_1(a)$ and variance (always) bounded by $1/4$. \square

Assuming that B has smoothness of order $s > 0$ around a , in a Hölder sense for instance, we then have $\mathfrak{b}_h(f_1)(a) \lesssim h^s$ as soon as $\ell \geq s - 1$, and therefore the estimator $|\mathcal{U}_1|^{-1} \sum_{u \in \mathcal{U}_1} K_h(a - \zeta_u)$ has pointwise squared risk of order $h^{2s} + (nh)^{-1}$ in the following sense:

$$\left(\inf_{h>0} (h^s + (nh)^{-1/2}) \right)^{-1} (\widehat{B}_{n,h}(a) - B(a))$$

is bounded in probability as $n \rightarrow \infty$.

Finding the optimal bandwidth h leads to the classical rate $\inf_{h>0} (h^s + (nh)^{-1/2}) \approx n^{-s/(2s+1)}$ in nonparametric estimation, which is always a slower rate of convergence than $n^{-1/2}$. Combining the two estimates (4.7) and (4.8) for an optimal bandwidth, we see that $\widehat{B}_{n,h}(a)$ estimates $B(a)$ with optimal (normalised) order $n^{-s/(2s+1)}$. These are classical results in nonparametric estimation, see *e.g.* [96, 97] and the references therein, in particular regarding data driven choices of h , since the smoothness $s > 0$ is only a mathematical construct that has no real meaning in practice.

Individual dynamics data, stochastic viewpoint, population observation. Following in spirit Section 3.2 but now with data extracted from \mathcal{U}_2 , we first look for the behaviour of empirical sums of the form

$$\mathcal{E}^T(g, \mathcal{U}_2) = \frac{1}{|\mathcal{U}_2|} \sum_{u \in \mathcal{U}_2} g(\zeta_u),$$

for nice (say bounded) test functions $g : [0, \infty) \rightarrow \mathbb{R}$. As in Section 3.2, we also have a many-to-one formula that now reads

$$\mathbb{E} \left[\sum_{u \in \mathcal{U}_2} g(\zeta_u^T) \right] = \mathbb{E} \left[\sum_{u \in \mathcal{U}_2} g(\zeta_u) \right] = 2^{-1} \int_0^T e^{\lambda_2 s} \mathbb{E} [g(\tilde{\chi}_s) H_B(\tilde{\chi}_s)] ds, \quad (4.9)$$

where $(\tilde{\chi}_t)_{t \geq 0}$ is the auxiliary one-dimensional auxiliary Markov process with generator \mathcal{A}_{H_B} , see (3.9), where H_B is characterised by (3.11) above. Assuming again ergodicity, we approximate the right-hand side of (4.9) and

obtain (at least heuristically)

$$\begin{aligned}\mathbb{E}\left[\sum_{u \in \mathcal{U}_2} g(\zeta_u)\right] &\sim c_B 2^{-1} \frac{e^{\lambda_2 T}}{\lambda_2} \int_0^\infty g(x) H_B(x) e^{-\int_0^x H_B(u) du} dx \\ &= c_B \frac{e^{\lambda_2 T}}{\lambda_2} \int_0^\infty g(x) e^{-\lambda_2 x} f_1(x) dx.\end{aligned}$$

since $H_B(x) \exp(-\int_0^x H_B(y) dy) = 2e^{-\lambda_2 x} f_1(x)$ by (3.11). We again have an approximation of the type $\mathbb{E}[|\mathcal{U}_2|] \sim \kappa_B e^{\lambda_2 T}$ with another constant κ'_B and we eventually expect

$$\mathcal{E}^T(g, \mathcal{U}_2) \sim \mathring{\mathcal{E}}(g) := \frac{c_B}{\lambda_2 \kappa'_B} \int_0^\infty g(x) e^{-\lambda_2 x} f_1(x) dx = 2 \int_0^\infty g(x) e^{-\lambda_2 x} f_1(x) dx$$

as $T \rightarrow \infty$, where the last equality stems from the identity $c_B = 2\lambda_2 \kappa'_B$ that can be readily derived by picking $g = 1$ and using (3.11) together with the fact that f_2 is a density function.

Proposition 4.2: (*Rate of convergence for particles living at time T - Theorem 4 in [14]*) Assume $\lambda_2 \leq 2 \inf_x H_B(x)$, and B differentiable satisfying $B'(x) \leq B(x)^2$ and $0 < c \leq B(x) \leq 2c$ for every $x \geq 0$ and some $c > 0$. Then

$$e^{\lambda_2 T/2} (\mathcal{E}^T(g) - \mathring{\mathcal{E}}(g))$$

is asymptotically bounded in probability.

Estimation: Step 1). Reconstruction formula for $B(a)$. We have

$$B(a) = \frac{f_1(a)}{1 - \int_0^a f_1(y) dy} = \frac{2^{-1} f_2(a) e^{\lambda_2 a}}{1 - 2^{-1} \int_0^a f_2(y) e^{\lambda_2 y} dy} \quad (4.10)$$

and from the definition $\mathring{\mathcal{E}}(g) = 2 \int_0^\infty g(x) e^{-\lambda_2 x} f_1(x) dx$ we obtain the formal reconstruction formula

$$B(a) = \frac{\mathring{\mathcal{E}}(2^{-1} e^{\lambda_2 \cdot} \delta_a(\cdot))}{1 - \mathring{\mathcal{E}}(2^{-1} e^{\lambda_2 \cdot} \mathbf{1}_{\{\cdot \leq a\}})} \quad (4.11)$$

where $\delta_a(\cdot)$ denotes the Dirac function at x . Therefore, taking g as a weak approximation of δ_a via a kernel, we obtain a strategy for estimating $B(a)$ replacing $\mathring{\mathcal{E}}(\cdot)$ by its empirical version $\mathcal{E}^T(\mathcal{U}_2, \cdot)$.

Estimation: Step 2). Construction of a kernel estimator and function spaces . Let $K : [0, \infty) \rightarrow \mathbb{R}$ be a kernel function. For $h > 0$, set $K_h(x) = h^{-1}K(h^{-1}x)$. In view of (4.11), we define the estimator

$$\widehat{B}_{T,h}(a) = \frac{\mathcal{E}^T(\mathcal{U}_2, 2^{-1}e^{\lambda_2 \cdot} K_h(a - \cdot))}{1 - \mathcal{E}^T(\mathcal{U}_2, 2^{-1}e^{\lambda_2 \cdot} \mathbf{1}_{\{\cdot \leq a\}})} \quad (4.12)$$

on the set $\mathcal{E}^T(\mathcal{U}_2, 2^{-1}e^{\lambda_2 \cdot} \mathbf{1}_{\{\cdot \leq a\}}) \neq 1$ and 0 otherwise. Thus $\widehat{B}_{T,h}(a)$ is specified by the choice of the kernel K and the bandwidth $h > 0$.

Performances of the Estimator. We are ready to give the rate of convergence of $\widehat{B}_T(a)$ for a restricted to a compact interval \mathcal{D} , uniformly over Hölder balls $\mathcal{H}_{\mathcal{D}}^s$

Proposition 4.3: (Upper rate of convergence, Theorem 7 in [14])
In the same setting as in Proposition 4.2, specify $\widehat{B}_{T,h}$ with a kernel satisfying (4.5) for some $\ell > 1$ and

$$h = \widehat{h}_T = \exp\left(-\frac{1}{2s+1}\lambda_2 T\right)$$

for some $s \in (1, \ell + 1)$. Then

$$e^{\lambda_2 \frac{s}{2s+1} T} (\widehat{B}_{T,h}(a) - B(a))$$

is asymptotically bounded in probability if B is s -Hölder in a neighbourhood of a .

This rate is indeed optimal in a minimax sense, see Theorem 8 in [14], where the problem of estimating λ_2 is also considered. The proof of Proposition 4.3 is detailed in [14]. In a more condensed way, they can also be found in [98].

Individual dynamics data, deterministic viewpoint. In the field of "deterministic" inverse problems, we model the noise by assuming that we observe data in a certain metric space up to an error ε according to this metric. In our case, this means that we first assume that the population has reached its steady asymptotic behaviour given by Theorem 3.6, and second that there exists a (known) noise level $\varepsilon > 0$, and that we observe the distribution of ages of dividing cells, defined by

$$f_k(a) := \frac{B(a)N_k(a)}{\int B(a)N_k(a)da},$$

up to a noise, *i.e.* the measurement $H_k^\varepsilon(a)$ is such that

$$\|f_k^\varepsilon - f_k\|_{W^{-s,p}([0,\infty))} \leq \varepsilon,$$

with $s \geq 0$, $1 \leq p \leq \infty$ and $W^{-s,p}([0, \infty))$ the corresponding Sobolev space. Integrating (3.3) to express $N_k(a)$ in terms of $B(a)N_k(a)$ and λ_k , chosen with $k = 1$ or $k = 2$ according to the observation scheme considered, we find the formula

$$B(a) = \frac{B(a)N_k(a)}{N_k(a)} = \frac{B(a)N_k(a)}{e^{-\lambda_k a} \int_a^\infty B(s)N_k(s)e^{\lambda_k s} ds} = \frac{f_k(a)}{e^{-\lambda_k a} \int_a^\infty f_k(s)e^{\lambda_k s} ds}, \quad (4.13)$$

where we recognize (4.4) if $k = 1$ and (4.11) if $k = 2$. This naturally leads us to define an estimate B_ε by replacing in this formula f_k by f_k^ε , and add a threshold condition for the denominator, as done above by considering compact intervals. If $s = 0$, *i.e.* if the noise lies in $L^p([0, \infty))$, we do not need to regularize this estimate: the problem is well-posed, and B_ε provides directly an estimate for B in a space $L^p([0, \infty))$ weighted by N_k . If either $s < 0$ or we want an estimate for B in some $W^{m,p}$ space with $m > 0$, then a regularization is needed: in exactly the same spirit as for kernel density estimation, we can define

$$f_k^{\varepsilon,h} = K_h * f_k^\varepsilon, \quad (4.14)$$

and we have the following result, deterministic version of the above Propositions 4.1 and 4.2.

Proposition 4.4: *Let K a kernel satisfying (4.5), $K \in C_b^1(\mathbb{R})$, and $K_h(\cdot) = 1/hK(\cdot/h)$. Let $1 \leq p \leq \infty$ and $\theta \in [0, 1]$. We have the estimate*

$$\|f_k^{\varepsilon,h} - f_k\|_{L^p} \leq \|K_h * f_k - f_k\|_{L^p} + C(K)h^{-\theta} \|f_k - f_k^\varepsilon\|_{W^{-\theta,p}},$$

where $C(k)$ is a constant depending only on the kernel K and on its derivative.

We do not specify here the standard machinery to obtain an estimate for B from the estimate for f_k : it consists in dividing $f_k^{\varepsilon,h}$ by N_k^ε - we do not need any regularisation for the denominator, thanks to the integral and to the choice $\theta \leq 1$ - and then thresholding. See for instance [99].

We then find that, for a noise ε in the space $W^{-\theta,p}$, *i.e.* if we have

$$\|f_k - f_k^\varepsilon\|_{W^{-\theta,p}} \leq \varepsilon,$$

and if we assume $f \in W^{s,p}$ with $\ell \geq s - 1$, the optimal estimate is in the order of $\varepsilon^{s/(s+\theta)}$, and achieved for $h \approx \varepsilon^{s/(s+\theta)}$. We first notice that if $\theta = 0$ (noise in L^2), this speed is of order ε : we do not need any regularisation, and we face a well-posed inverse problem!

We notice that this result is fully coherent with the statistical estimates of Propositions 4.1 and 4.2: to see it, the correct heuristics consists in taking $\theta = \frac{1}{2}$ (for a heuristics of the regularity of the empirical measure) and $\varepsilon = n^{-1/2}$ (the noise level being given by a central limit theorem), see [100] for an illuminating explanation of this comparison. We then have an estimate in the order of

$$\varepsilon^{s/(s+\theta)} = \varepsilon^{s/(s+1/2)} = n^{-s/(2s+1)},$$

as above. We further develop these heuristics or comparison between stochastic and deterministic noise in Section 4.2.2 below.

Finally, we note that the proof of Proposition 4.4 is not more involved for $k = 2$ than for $k = 1$, contrarily to the stochastic setting where the selection bias and the dependence between the individuals in the population case make it much more complex.

4.1.2. Population point data

Let us imagine that we are given a noisy measurement of the distribution of cells $N_k(a)$. This noise may be modeled by three different settings, increasingly realistic:

1. deterministic noise model: we model the noise by a measurement N_k^ε such that

$$\|N_k^\varepsilon - N_k\|_{W^{-s,p}([0,\infty))} \leq \varepsilon.$$

2. Stochastic sampling noise: we assume that we observe a sample of ages a_1, \dots, a_n realisations of A_1, \dots, A_n *i.i.d.* random variables of density N_k . We could refine this setting by adding a measurement noise to each a_i .
3. Stochastic process: we observe, at a given time T , a sample of ages of cells. This means that we observe $\{a_u\}$, $u \in \mathcal{U}_3$ defined by

$$a_u = T - b_u, \quad u \in \mathcal{U}_3 = \{u \in \mathcal{U}, \quad b_u \leq T < b_u + \zeta_u\}.$$

For the third model, one first needs to establish asymptotic results as done in [14] given in Proposition 3.8 above for individual dynamics data. Having

$$\mathcal{E}(g) = 2\lambda_2 \int_0^\infty g(x) e^{-\lambda_2 x} \exp\left(-\int_0^x B(y) dy\right) dx$$

and ignoring the fact that λ_2 is unknown, we can anticipate that by picking a suitable test function g as a kernel, the information about $B(x)$ can only be inferred through $\exp(-\int_0^x B(y)dy)$. More precisely, consider the quantity

$$\widehat{f}_{h,T}(x) = -\mathcal{E}^T \left(\lambda_2 (K_h)'(x - \cdot) \right)$$

for a kernel satisfying (4.5). By Proposition 3.8 and integrating by part, we readily see that

$$\widehat{f}_{h,T} \mapsto -\mathcal{E} \left(\frac{1}{\lambda_2} (K_h)'(x - \cdot) \right) = \int_0^\infty K_h(x - y) f_{B+\lambda_2}(y) dy \quad (4.15)$$

in probability as $T \rightarrow \infty$, where $f_{B+\lambda_2}$ is the density associated to the division rate $B(x) + \lambda_2$. On the one hand, using following line by line the proofs of [14] it is not difficult to show that the rate of convergence in (4.15) is of order $h^{-3/2} e^{\lambda_2 T/2}$ since we take the derivative of the kernel K_h . On the other hand, the limit $\int_0^\infty K_h(x - y) f_{B+\lambda_2}(y) dy$ approximates $f_{B+\lambda_2}(x)$ with an error of order h^s if B is s -Hölder. Balancing the two error terms in h , we see that we can estimate $f_{B+\lambda_2}(x)$ with an error of (presumably optimal) order $\exp(-\lambda_2 \frac{s}{2s+3} T)$. Due to the fact that the denominator in representation (4.10) can be estimated with parametric error rate $\exp(-\lambda_2 T/2)$ (possibly up to polynomially slow terms in T), we end up with the rate of estimation $\exp(-\lambda_2 \frac{s}{2s+3} T)$ for $B(x)$ as well, and that can be related to an ill-posed problem of order 1 (see for instance [96]). This phenomenon, namely the structure of an ill-posed problem of order 1 in restriction to data alive at time T , appears in the other settings: for the estimation of a size-division rate from living cells at a given large time in [101, 99] or for the estimation of the dislocation measure for a homogeneous fragmentation, see [10].

For the first and second noise models, we use the explicit formula (3.5) to get

$$B(a) = -\lambda_k - \frac{\partial_a N_k(a)}{N_k(a)} \quad (4.16)$$

which is equivalent to (4.15). As for individual dynamics data, we see that we need to divide by the density, so that we will not be able to estimate B at places where it vanishes. The new fact is that, contrarily to Formula (4.13), the formula depends on the age-derivative of N_k , so that, as shown below in Proposition 4.5, the so-called *degree of ill-posedness* of the inverse problem is the one of estimating a function from its derivative: as for the third model, more regularisation is needed. We obtain the two following propositions.

Proposition 4.5: (Deterministic noise) Under the assumptions of Proposition 4.4, defining

$$H_{\varepsilon,h}(a) := -\lambda_k^\varepsilon N_k^\varepsilon(a) - (K_h * \partial_a N_k^\varepsilon)(a), \quad H(a) = B(a)N_k(a)$$

we have

$$\begin{aligned} \|H_\varepsilon - H\|_{L^p} &\leq C(K, N_k) (\|K_h * N_k - N_k\|_{L^p} \\ &\quad + |\lambda_k^\varepsilon - \lambda_k| + h^{-\theta-1} \|N_k^\varepsilon - N_k\|_{W^{-\theta,p}}) \end{aligned}$$

with $C(K, N_k)$ depending only on K, K' and N_k .

The proof is left to the reader; it is exactly the same ingredients as before, namely standard convolution inequalities. We see that for $N_k \in W^{s,p}$ and $\ell \geq s - 1$, and an error ε in $W^{-\theta,p}$, we have an optimal estimate in the order of $\varepsilon^{\frac{s}{s+\theta+1}}$, corresponding, for $\theta = 0$, to an inverse problem of degree of ill-posedness 1.

Proposition 4.6: (Stochastic sampling noise) Under the assumptions of Proposition 4.5, assume that we know λ_k from previous observations, and that we observe an i.i.d sample a_1, \dots, a_n of law N_k , and define the empirical measure

$$N_n(da) = \frac{1}{n} \sum_{i=1}^n \delta_{a_i}(da)$$

and its regularisation

$$N_{n,h}(a)da = K_h * \left(\frac{1}{n} \sum_{i=1}^n \delta_{a_i}(da) \right) = \frac{1}{n} \sum_{i=1}^n K_h(a - a_i)da$$

We define

$$H_{n,h}(a) := -\lambda_k - N_{n,h}(a) - \partial_a N_{n,h}(a), \quad H(a) := B(a)N_k(a),$$

and the bias

$$\mathfrak{b}_h(N_k)(a) = |(K_h * N_k)(a) - N_k(a)|.$$

We have the following estimate

$$\mathbb{E} [|H_{n,h}(a) - H(a)|^2] \leq \mathfrak{b}_h(N_k)(a)^2 + C(N_k, K) \frac{1}{nh^3}, \quad (4.17)$$

where $C(B, K)$ depends only on N_k, K and K' .

The proof is close to the proof of Proposition 4.1. The inflation in the variance term from the order $(nh)^{-1}$ to $(nh^3)^{-1}$ comes from the fact that we take a derivative $\partial_a N_{n,h}(a)$ of the kernel estimator $N_{n,h}(a)$. As previously seen, the bias is of order h^s if $N_k \in W^{s,p}$ and $\ell \geq s - 1$; this leads to an optimal error (*i.e.* the square root of the left-hand side in (4.17)) in the order of $n^{-\frac{s}{2s+3}}$. Taking in Proposition 4.5 $\theta = 1/2$ and $\varepsilon = n^{-1/2}$, we have $\varepsilon^{\frac{s}{s+3/2}} = n^{-\frac{s}{2s+3}}$: here again, this is the same optimal speed of convergence.

All these orders of magnitude for the convergence rates remain true for the size-structured model studied below.

4.2. Estimating a size-dependent division rate

We now review the methods and results developed to estimate a size-dependent division rate, as built in Section 2.3 and analysed in Section 3.3. We follow the same notations as above. We do not treat here the interesting question of estimating the fragmentation kernel $b(y, x)$, and refer for instance to [102, 9, 103, 10].

4.2.1. Individual dynamics data

Combining stochastic, deterministic and asymptotic approaches allows us to obtain easily reconstruction formulae.

Let us first revisit heuristically the formulae of [37, 19]. In general terms, we observe

$$\{(\xi_u, \chi_u, \zeta_u), u \in \mathcal{U}_k\}, \quad k = 1 \text{ or } k = 2, \quad \text{or} \quad \{\xi_u^T, u \in \mathcal{V}_T\},$$

with (ξ_u, χ_u, ζ_u) respectively the size at birth, size at division and lifetime of the individual u taken in the sample \mathcal{U}_k defined by (4.1) and (4.2), \mathcal{V}_T defined by (3.8) and ξ_u^T the size of the individual $u \in \mathcal{V}_T$ alive at time T . \mathcal{U}_1 models the genealogical observation and individual dynamics data, \mathcal{U}_2 the population observation and individual dynamics data, and \mathcal{V}_T population point data and population observation.

Assuming that the asymptotic behaviour of Section 3.3 has been reached in each of these models, we can interpret the densities with the help of Equation (3.16).

- $\xi_u, u \in \mathcal{U}_k$, has a density distribution given by

$$f_k^b(x) = \frac{k \int_x^\infty B(y) \tau(y) b(y, x) N_k(y) dy}{k \int_0^\infty \int_s^\infty B(y) \tau(y) b(y, s) N_k(y) dy ds} = \frac{\int_x^\infty B(y) \tau(y) b(y, x) N_k(y) dy}{\int_0^\infty B(y) \tau(y) N_k(y) dy}.$$

This formula is obtained by identifying the last term in (3.16) with the newborn proportion, and normalise it to obtain a density.

- χ_u , $u \in \mathcal{U}_k$, has density distribution given by

$$f_k^d(x) = \frac{B(x)\tau(x)N_k(x)}{\int_0^\infty B(y)\tau(y)N_k(y)dy}.$$

- ξ_u^T has for density N_k .

To estimate B , we can then write

$$B(x) = \frac{f_k^d(x)}{\tau(x)N_k(x)} \int_0^\infty B(y)\tau(y)N_k(y)dy,$$

and it remains to find formulae for τN_k and for $\int_0^\infty B(y)\tau(y)N_k(y)dy$.

Case $k = 1$ (genealogical observation). We denote $C = \int_0^\infty B(y)\tau(y)N_1(y)dy$ and write (3.16) as

$$\partial_x(\tau N_1) + C f_1^d = C f_1^b \implies \frac{\tau(x)N_1(x)}{C} = \int_x^\infty (f_1^d(y) - f_1^b(y)) dy,$$

so that we obtain the reconstruction formula

$$B(x) = \frac{f_1^d(x)}{\int_x^\infty (f_1^d(y) - f_1^b(y)) dy}. \quad (4.18)$$

Case $k = 2$ (population observation). We then have $\int_0^\infty B(y)\tau(y)N_2(y)dy = \lambda_2$, and (3.16) may be written as

$$\lambda_2 N_2 + \partial_x(\tau N_2) + \lambda_2 f_2^d = 2\lambda_2 f_2^b,$$

from which we deduce

$$\frac{\tau(x)N_2(x)}{\lambda_2} = \int_x^\infty (f_2^d(y) - 2f_2^b(y)) e^{\lambda_2 \int_x^y \frac{ds}{\tau(s)}} dy,$$

leading finally to the reconstruction formula

$$B(x) = \frac{f_2^d(x)}{\int_x^\infty (f_2^d(y) - 2f_2^b(y)) e^{\lambda_2 \int_x^y \frac{ds}{\tau(s)}} dy}. \quad (4.19)$$

Using either (4.18) or (4.19) and replacing f_k^d and f_k^b by the empirical distribution obtained from samples (ξ_i^b, ξ_i^d) , we can estimate B without any knowledge on the fragmentation kernel b , , as soon as both newborn and dividing cells distributions are observed. For genealogical data ($k = 1$), even the growth rate τ may be unknown. This remark may be generalised to other models, see for instance the formula (14) of [37] for a model with $k = 1$, the mitosis kernel (for which we have the simplification $f_k^b(x) = 2f_k^d(2x)$) and variable growth rates.

Individual dynamics data, stochastic approach, genealogical observation In the cases where we model the noise either deterministically or through an *i.i.d* sample, the reconstruction formulae (4.18) and (4.19) immediately yield estimation results similar to the ones of Propositions 4.4 and 4.1 stated for the age model. More involved is the case where we do not depart from (3.16) but from the stochastic model; it has been studied in [37] for the case of genealogical observation, easier to study than the population observation case. To our best knowledge, the solution for population observation, with all the difficulties we already mentioned for the age problem (selection bias, censoring, non-ancillarity) plus a more intricate model, remains open.

In this setting, we look for a nonparametric estimator of $x \mapsto B(x)$ using the observation scheme \mathcal{U}_1 defined in Section 4.1.1 We thus observe

$$(\xi_u)_{u \in \mathcal{U}_1} \quad \text{and} \quad (\zeta_u)_{u \in \mathcal{U}_1}.$$

We have (see Section 2.1)

$$\mathbb{P}(\chi_u \in (x, x + dx) | \chi_u \geq x) = B(x)dx = \tau(x)B(x)dt,$$

$$\mathbb{P}(\chi_u \geq x | \xi_u) = \mathbb{1}_{\{x \geq \xi_u\}} \exp\left(-\int_{\xi_u}^x B(y)dy\right).$$

Hence we infer, taking the equal mitosis kernel so that $2\xi_u = \chi_{u^-}$,

$$\mathbb{P}(\xi_u \in (x', x' + dx') | \xi_{u^-} = x) = 2B(2x')\mathbb{1}_{\{2x' \geq x\}} \exp\left(-\int_x^{2x'} B(y)dy\right)dx'.$$

We thus obtain a simple and explicit representation for the transition kernel $\mathcal{P}_B(x, dx') = \mathcal{P}_B(x, x')dx'$ as

$$\mathcal{P}_B(x, x') = 2B(2x')\mathbb{1}_{\{2x' \geq x\}} \exp\left(-\int_x^{2x'} B(y)dy\right).$$

Under appropriate conditions on B set out in details below, there exists a unique invariant probability $\nu_B(dx) = \nu_B(x)dx$ on $[0, \infty)$ such that the following contraction property holds

$$\sup_{|g| \leq V} \left| \mathcal{P}_B^k g(x) - \int_0^\infty g(z)\nu_B(z)dz \right| \leq RV(x)\gamma^k \quad (4.20)$$

(where, for an integer $k \geq 1$, we set $\mathcal{P}_B^k = \mathcal{P}_B^{k-1} \circ \mathcal{P}_B$) for an appropriate Lyapunov function V and some (explicitly computable) $\gamma < 1$. The proof

of (4.20) goes along a classical scheme and is detailed in Proposition 4 of [10], and for $\tau(x) = \kappa x$ (4.20) holds with

$$V(x) = \exp\left(\frac{m}{\kappa\mu}x^\mu\right)$$

for $\mu > 0$. Expand further the equation $\nu_B \mathcal{P}_B = \nu_B$:

$$\begin{aligned} \nu_B(y) &= \int_0^\infty \nu_B(x) \mathcal{P}_B(x, y) dx \\ &= 2B(2y) \int_0^{2y} \nu_B(x) \exp\left(-\int_x^{2y} B(y') dy'\right) dx \\ &= 2B(2y) \int_0^\infty \int_0^\infty \mathbf{1}_{\{x \leq 2y, y' \geq y\}} \nu_B(x) \mathcal{P}_B(x, y') dy' dx. \end{aligned}$$

This yields the key representation

$$\nu_B(y) = 2B(2y) \mathbb{P}_{\nu_B}(\xi_{u^-} \leq 2y, \xi_u \geq y).$$

We conclude

$$B(y) = \frac{1}{2} \frac{\nu_B(y/2)}{\mathbb{P}_{\nu_B}(\xi_{u^-} \leq y, \xi_u \geq y/2)} \quad (4.21)$$

and this yields the estimator

$$\widehat{B}_{n,h}(y) = \frac{1}{2} \frac{n^{-1} \sum_{u \in \mathcal{U}_{[n]}} K_h(\xi_u - y/2)}{n^{-1} \sum_{u \in \mathcal{U}_{[n]}} \mathbf{1}_{\{\xi_{u^-} \leq y, \xi_u \geq y/2\}} \sqrt{\varpi_n}},$$

where the kernel $K_h(y) = h^{-1}K(h^{-1}y)$ is specified with an appropriate bandwidth (and technical threshold $\varpi_n > 0$).

We assess the quality of \widehat{B}_n in squared-loss error over compact intervals \mathcal{D} . We need to specify local smoothness properties of B over \mathcal{D} , together with general properties that ensure that the empirical measurements converge with an appropriate speed of convergence. This amounts to impose an appropriate behaviour of B near the origin and infinity.

For $\alpha > 0$ and positive constants r, m, ℓ, L , introduce continuous functions $B : [0, \infty) \rightarrow [0, \infty)$ such that

$$\int_0^{r/2} x^{-1} B(2x) dx \leq L, \quad \int_{r/2}^r x^{-1} B(2x) dx \geq \ell, \quad B(x) \geq m x^\alpha \text{ for } x \geq r. \quad (4.22)$$

Define

$$\delta := \frac{1}{1 - 2^{-\alpha}} \exp\left(-\left(1 - 2^{-\alpha}\right) \frac{m}{\kappa\alpha} r^\alpha\right).$$

Let γ denote the spectral radius of the operator $\mathcal{P}_B - 1 \otimes \nu_B$ acting on the Banach space of functions $g : [0, \infty) \rightarrow \mathbb{R}$ such that

$$\sup\{|g(x)|/V(x), x \geq 0\} < \infty.$$

Assumption 2: We have $\delta < \frac{1}{2}$ and $\gamma < 1$.

It is possible to obtain bounds on r, m, ℓ, L so that Assumption 2 holds, by using explicit bounds on γ following Hairer and Mattingly [104], see also Baxendale [105]. We are ready to state the performance of the estimator.

Theorem 4.7: (*Adapted from Theorem 2 from [37]*) Specify $\widehat{B}_{n,h}$ with a kernel K satisfying Assumption 4.5 for some $n_0 > 0$ and

$$h = n^{-1/(2s+1)}, \quad \varpi_n \rightarrow 0.$$

For every compact interval $\mathcal{D} \subset (0, \infty)$ such that $\inf \mathcal{D} \geq r/2$, there exists a choice of m, ℓ, L, α such that Assumption 2 is satisfied. For B s -Hölder satisfying (4.22), we have

$$\mathbb{E}_\mu [\|\widehat{B}_n - B\|_{L^2(\mathcal{D})}^2]^{1/2} \lesssim \varpi_n^{-1} n^{-s/(2s+1)},$$

where $\mathbb{E}_\mu[\cdot]$ denotes expectation with respect to any initial distribution $\mu(dx)$ for ξ_\emptyset on $(0, \infty)$ such that $\int_0^\infty V(x)^2 \mu(dx) < \infty$.

We illustrate this result in Fig. 9 for the reconstruction of a rate $x B(x) = x^2$. Since ϖ_n is arbitrary, we obtain the classical rate $n^{-s/(2s+1)}$ which is optimal in a minimax sense for density estimation. It is optimal in our context, using for instance the results of [106]. The knowledge of the smoothness s that is needed for the construction of \widehat{B}_n is not realistic in practice. An adaptive estimator could be obtained by using a data-driven bandwidth in the estimation of the invariant density $\nu_B(y/2)$ in (4.21). The Goldenschluger-Lepski bandwidth selection method seen in this context [99] would presumably yield adaptation. Finally, let us revisit the representation formula

$$B(y) = \frac{1}{2} \frac{\nu_B(y/2)}{\mathbb{P}_{\nu_B}(\xi_{u^-} \leq y, \xi_u \geq y/2)}$$

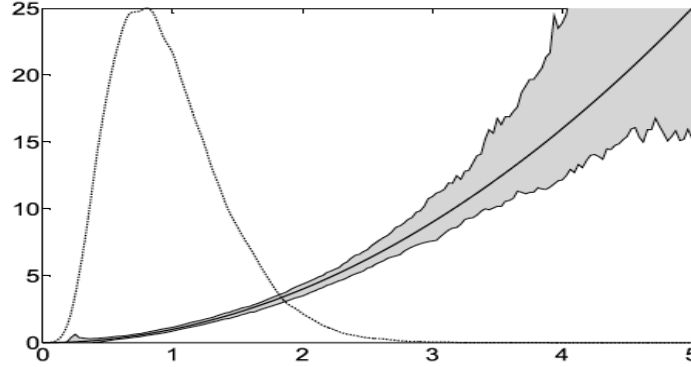


Fig. 9. Reconstruction for $n = 2^{10}$, error band for 95%, 100 simulations, with a small threshold $\varpi_n = 1/n$. We see that the error grows larger as x grows larger, as expected since the density of cells vanishes. Fig. 3 from [37].

by noticing that we always have $\{\xi_{u^-} \geq y\} \subset \{\xi_u \geq y/2\}$, hence

$$\begin{aligned} \mathbb{P}_{\nu_B}(\xi_{u^-} \leq y, \xi_u \geq y/2) &= \mathbb{P}_{\nu_B}(\xi_u \geq y/2) - \mathbb{P}_{\nu_B}(\xi_{u^-} \geq y) \\ &= \int_{y/2}^{\infty} \nu_B(x) dx - \int_y^{\infty} \nu_B(x) dx \\ &= \int_{y/2}^y \nu_B(x) dx. \end{aligned}$$

Finally, for constant growth rate, we obtain

$$B(y) = \frac{1}{2} \frac{\nu_B(y/2)}{\int_{y/2}^y \nu_B(x) dx},$$

where we recognize (4.18). The “gain” in the convergence rate $n^{-s/(2s+1)}$ versus the rate $n^{-s/(2s+3)}$ obtained in the proxy model based on the transport-fragmentation equation, as seen in Section 4.1 for the age model, comes from the fact that we estimate the invariant measure “at division” versus the invariant measure “at fixed time” in the proxy model. In other words, there is more “nonparametric statistical information” in data extracted from \mathcal{U}_2 rather than \mathcal{V}_T , regardless of the tree structure. However $|\mathcal{V}_T| \approx |\mathcal{U}_2|$ as stems from the supercritical branching process structure.

4.2.2. Population point data

We now turn to the case of less rich observation schemes, where we only have access to population point data, which relate to the eigenvector solution N_k .

For the noise, we consider either a deterministic noise or a sampling noise: as for the individual dynamics case, a complete approach, which would depart from the stochastic branching tree, has not yet been carried out.

Contrarily to the case of individual dynamics data, the shape of the fragmentation kernel is important here, and needs to be previously known, as well as the Malthusian parameter λ_k and the growth rate τ .

Estimating the division rate B may be formulated by the following inverse problem.

We know *a priori* the growth rate τ , the fragmentation kernel $b(y, x) = \frac{1}{y}b_0(\frac{x}{y})$ and the Malthusian parameter λ_k , and measuring either N_k^ε (deterministic noise) such that

$$\|N_k^\varepsilon - N_k\|_{W^{-s,p}([0,\infty))} \leq \varepsilon,$$

or a sample x_1, \dots, x_n realisations of X_1, \dots, X_n *i.i.d.* random variables of law N_k (sampling noise), with (N_k, λ_k) solution to (3.16) *i.e.*

$$\begin{cases} \frac{\partial}{\partial x}(\tau N_k(x)) + \lambda_k N(x) = -(\tau B N_k)(x) + k \int_0^1 (\tau B N_k)(\frac{x}{z}) \frac{b_0(dz)}{z}, \\ \tau N_k(0) = 0, \end{cases} \quad (4.23)$$

How to estimate B ?

We notice the same ingredients as for the age model: 1/ B appears in the equation only multiplied by τN_k , so that we cannot estimate it at places where τN_k vanishes; 2/ the equation displays a size-derivative of N_k , so that we expect an inverse problem of degree of ill-posedness one as in Section 4.1.2; 3/ replacing the unknown B by the density of dividing cells $B N_k$, we transform a nonlinear inverse problem into a linear one.

However, contrarily to the simple age model, we do not have any explicit formula here: a dilation operator needs to be inverted. We decompose (4.23) into

$$L(N_k) = G_k(B \tau N_k) \quad \text{with} \quad G_k(f)(x) := k \int_0^1 f(\frac{x}{z}) \frac{b_0(dz)}{z} - f(x), \quad (4.24)$$

$$L(N_k) := \partial_x(\tau N_k) + \lambda_k N_k,$$

and estimate B through the following steps:

- Solve $G_k(f) = L$ for f , L in suitable spaces: for simplicity of inversion formulae, we thus choose Hilbert spaces of type $L^2([0, \infty), x^p dx)$ [107].

Note that under this shape, the problem to solve $N_k \rightarrow f = B\tau N_k$ is now linear.

- Estimate $L(N_k)$ from the measurement in the chosen space: to do so, we can either depart from N_k^ε or from a statistical sample, and then divide by (an estimate of) N_k and threshold appropriately.

The second step is exactly the same as what has been done in Section (4.1) for the renewal equation, so that we will not detail this part anymore here, and focus on the first step, which is specific to the growth-fragmentation equation.

Solving a dilation equation

The first step consists in inverting the dilation operator G_k defined by (4.24). We begin to treat the equal mitosis case, first studied by B. Perthame and J. Zubelli [12, 101, 99], and then turn to more general fragmentation kernels [108].

For the equal mitosis or diagonal kernel $b_0(x) = \delta_{x=\frac{1}{2}}$, we have the following result.

Proposition 4.8: (*Adapted from Theorem A.3. of [101]*) *Let G_k defined by (4.24), $b_0(x) = \delta_{x=\frac{1}{2}}$, $L \in L^2(x^p dx)$ with $p \neq 2k - 1$.*

There exists a unique solution $f \in L^2(x^p dx)$ to

$$G_k(f) = 2kf(2\cdot) - f(\cdot) = L,$$

and this solution depends continuously on $\|L\|_{L^2(x^p dx)}$. Moreover, defining

$$H_k^0 := \sum_{j=1}^{\infty} (2k)^{-j} L(2^{-j}x), \quad H_k^\infty := - \sum_{j=0}^{\infty} (2k)^j L(2^jx),$$

we have $f = H_k^0$ if $p < 2k - 1$ and $f = H_k^\infty$ if $p > 2k - 1$. If $L \in L^q$ then $H_0 \in L^q$ for any $1 \leq q \leq \infty$.

For $L = 0$, any distribution of the form $f(\frac{\ln x}{x^2})$ with $f \in \mathcal{D}'([0, \infty))$ $\ln - 2$ periodic is solution.

Proof: The proof is based on the Lax-Milgram theorem applied to the bilinear forms

$$\begin{cases} a_p(u, v) = \int (-2ku(2x) + u(x)) v(x) x^p dx, \\ b_p(u, v) = \int (2ku(2x) - u(x)) v(2x) x^p dx, \end{cases}$$

and by Cauchy-Schwarz inequality, a_p and b_p are respectively coercive for $p > p_k$ and $p < p_k$ with $p_1 = 1$ and $p_2 = 3$. \square

In this result, we first notice that uniqueness depends on the space chosen: there is no reason, generally speaking, to have $H_k^0 = H_k^\infty$, so that departing from an estimate $L(N_k^\varepsilon)$, we have infinitely many choices. We first restrict to the two solutions H_k^0 and H_k^∞ , since the others do not vanish fast enough at infinity compared to the one we look for, recall Theorem 3.9. Among these two solutions, H_k^0 "behaves better" at infinity, and H_k^∞ at zero, hence in [108] we proposed a combination of both solutions as a best approximation in $L^2((x^p + 1)dx)$ for $p > 3$, namely, for a given L , we define

$$H_k^{\bar{x}} = H_k^0 \mathbb{1}_{\{x \leq \bar{x}\}} + H_k^\infty \mathbb{1}_{\{x > \bar{x}\}}. \tag{4.25}$$

This solution is no more an exact solution of $G_k(f) = L$ unless $H_k^0 = H_k^\infty$. However, this property being satisfied for the "true" underlying distribution, it defines a convenient approximation as shown below.

For general self-similar fragmentation kernels, we use the Mellin transform - an important tool for the study of the equation in many cases, see [83, 64]. We recall that the Mellin transform \mathcal{M} is an isometry between $L^2(x^q dx)$ and $L^2(\frac{q+1}{2} + i\mathbb{R})$ defined by

$$\mathcal{M}[f](s) := \int_0^\infty x^{s-1} f(x) dx, \quad \mathcal{M}_q^{-1}[F](x) := \int_{-\infty}^\infty x^{-\frac{q+1}{2}-iv} F(\frac{q+1}{2} + iv) dv. \tag{4.26}$$

The Mellin transform for the operator G_k is then

$$\mathcal{M}[\mathcal{G}(f)](s) = (k\mathcal{M}[b_0](s) - 1)\mathcal{M}[f](s),$$

and we see that, if $|k\mathcal{M}[b_0](s) - 1|$ is bounded from below by a positive constant on the integration line $\frac{q+1}{2} + i\mathbb{R}$, we can define the inverse

$$H_k^q := \mathcal{M}_q^{-1} \left[\frac{\mathcal{M}[\mathcal{G}(f)](s)}{k\mathcal{M}[b_0](s) - 1} \right]. \tag{4.27}$$

We notice that for $s_k = k$ we have $k\mathcal{M}[b_0](s_k) - 1 = 0$. This zero, together with the isometry given by (4.26) and the inversion formula (4.27), gives insight on why $p_k = 2k - 1$ is the pivot in Proposition 4.8 (we have $s_k = \frac{p_k+1}{2}$), and why $H_k^q \neq H_k^{q'}$ if $q < s_k < q'$: the residue theorem quantifies exactly their difference, see Proposition 4 in [108] for more details.

Estimate with a deterministic noise Let us assume here that we measure N_k up to a deterministic noise of level $\varepsilon > 0$, $0 \leq \theta < 1$:

$$\|N_k - N_k^\varepsilon\|_{H^{-\theta}([0, \infty))} \leq \varepsilon.$$

By the general theory of linear inverse problems, let us pick any regularisation method of optimal order [107], of parameter $h > 0$, and define an

approximation $L(N_k^\varepsilon)_h$ such that, for $N_k \in H^m([0, \infty))$, and $q > 2k - 1$, we have

$$\|L(N_k^\varepsilon)_h - L(N_k)\|_{L^2((1+x^q)dx)} \leq C\left(\frac{\varepsilon}{h} + h^m\right),$$

with C depending only on the method chosen and on the norm of N_k in H^m . Since we want to estimate $H_k = BN_k$ in $L^2((1+x^q)dx)$ with $q > 2k - 1$, we define for some $a > 0$

$$H_{\varepsilon,h} := \mathcal{M}_0^{-1} \left[\frac{\mathcal{M}[L(N_k^\varepsilon)_h](s)}{k\mathcal{M}[b_0](s) - 1} \right] \mathbb{1}_{\{x \leq a\}} + \mathcal{M}_q^{-1} \left[\frac{\mathcal{M}[L(N_k^\varepsilon)_h](s)}{k\mathcal{M}[b_0](s) - 1} \right] \mathbb{1}_{\{x > a\}} \quad (4.28)$$

and we get the following proposition.

Proposition 4.9: (Adapted from [108], Theorem 1.1.) For $N \in H^m([0, \infty))$ solution to the eigen equation (4.23) we have

$$\|N - N_\varepsilon\|_{H^{-\theta}([0, \infty))} \leq \varepsilon \implies \|H_{\varepsilon,h} - BN_k\|_{L^2((1+x^q)dx)} \leq C\left(\frac{\varepsilon}{h^{1+\theta}} + h^m\right)$$

where C depends only on $\|N\|_{H^m}$ and the regularisation method chosen.

Estimation with a stochastic noise Let us now assume that we observe a sample of n cells, of sizes x_1, \dots, x_n , that are realisations of

$$(X_1, \dots, X_n),$$

where the X_i are independent, with common density distribution $N(x)dx$ (recall that we have $N \geq 0$ and that we pick the normalisation $\int_0^\infty N = 1$). From (4.24), we have the formal representation

$$B = \frac{(G_k)^{-1}(L(N_k))}{\tau N_k}.$$

Thus, from data (X_1, \dots, X_n) we can build a regularisation

$$\widehat{N}_{h,k} = \frac{1}{nh} \sum_{i=1}^n K_h(\cdot - X_i)$$

which simply amounts to have a convolution of the empirical measure $n^{-1} \sum_{i=1}^n \delta_{X_i}(dx)$ with a well behaved kernel $K_h(\cdot) = h^{-1}K(h^{-1}\cdot)$. The resulting $\widehat{N}_{h,k}$ being smooth (by picking K smooth enough), we may compute the action of the differential operator L on \widehat{N}_h . As soon as the operator G_k has bounded inverse, or that a nice approximation $(\mathfrak{G}_k)^{-1}$ of $(G_k)^{-1}$ is available, we may form the simple estimator:

$$\widehat{B}_{n,h} = \frac{(\mathfrak{G}_k)^{-1}(L(\widehat{N}_{h,k}))}{\tau \widehat{N}_{h,k}}. \quad (4.29)$$

In [99], we realise this program for the binary fragmentation operator and we propose a method to automatically select the bandwidth h from data. The following kind of results can be obtained: for a compact set \mathcal{D} , one can construct an approximation $(\mathfrak{G}_k)^{-1}$ and select a bandwidth h such that if $B \in H^s$, then

$$\mathbb{E} [\|\widehat{B}_{n,h} - B\|_{L^2(\mathcal{D})}] \lesssim n^{-s/(2s+3)}. \quad (4.30)$$

We obtain the rate of convergence that corresponds to ill-posed problem of order 1, and this is consistent with the other approaches based on large population data (here of size n) alive at a given fixed, (but large) time.

Comparing deterministic and stochastic methods

The stochastic method rate of convergence $n^{-s/(2s+3)}$ for ill-posed problems of degree 1 in the statistical minimax theory [97] is to be compared with the deterministic method rate $\epsilon^{s/(s+1)}$, as stems from the classical theory exposed for instance in the classical textbook [107]. These are actually the same results, as stems from a classical analysis of comparison between stochastic and deterministic ill-posed inverse problems, see the illuminating paper [100].

Suppose we have an approximate knowledge of N and λ up to deterministic errors $\zeta_1 \in L^2$ and $\zeta_2 \in \mathbb{R}$ with noise level $\epsilon > 0$: we observe

$$N_\epsilon = N + \epsilon\zeta, \quad \|\zeta\|_{L^2} \leq 1, \quad (4.31)$$

and

$$\lambda_\epsilon = \lambda + \epsilon\zeta_2, \quad |\zeta_2| \leq 1. \quad (4.32)$$

From the formal representation

$$B = \frac{(G_k)^{-1}(L(N_k))}{\tau N_k},$$

The recovery of $L(N_k)$ is ill-posed in the terminology of Wahba [109] since it involves the computation of the derivative of N . If G_k is bounded with an inverse bounded in L^2 and the dependence in λ is continuous, the overall inversion problem is ill-posed of degree $a = 1$. By classical inverse problem theory for linear cases (here the problem is non linear), this means that if $N \in W^{s,2}$, the optimal recovery rate in L^2 -error norm should be $\epsilon^{s/(s+a)} = \epsilon^{s/(s+1)}$ (see also [12, 101]).

Suppose now that we replace the deterministic noise ζ_1 by a random Gaussian *white noise*: we observe

$$N_\varepsilon = N + \varepsilon \dot{W} = A \frac{\partial}{\partial x} N(x) dx + \varepsilon \dot{W} \quad (4.33)$$

where \dot{W} is a Gaussian white noise (a random distribution) and $A\varphi(x) = \int_0^x \varphi(y) dy$ denotes the integration operator (which has degree of ill-posedness $a = 1$). This setting is actually statistically (asymptotically) very close to observing (X_1, \dots, X_n) where the X_i are independent random variables, with common density N , at least over compact intervals \mathcal{D} and as soon as N does not degenerate, as follows from the celebrated result of Nußbaum [110].

In this setting, we want to recover $\frac{\partial}{\partial x} N$. Integrating, we equivalently observe

$$Y_\varepsilon(\cdot) = \int_0^\cdot A \frac{\partial}{\partial x} N(x) dx + \varepsilon \mathcal{W},$$

where $(\mathcal{W}_x, x \geq 0)$ is a Brownian motion. Applying formally the 1/2-fractional derivative operator $D^{1/2}$, we recast the observation Y_ε into an equivalent observation

$$Z_\varepsilon = D^{1/2} \int_0^\cdot A \frac{\partial}{\partial x} N(x) dx + \varepsilon D^{1/2} \mathcal{W},$$

so that $D^{1/2} \mathcal{W}$ is in L^2 . The operator $\varphi \mapsto D^{1/2} \int_0^\cdot A \varphi(x) dx$ maps L^2 onto $W^{1+1-1/2,2}$ *i.e.* we have an effective degree of ill-posedness $a = 3/2$. We should then obtain an optimal rate of the form

$$\varepsilon^{s/(s+3/2)} = \varepsilon^{2s/(2s+3)} = n^{-s/(2s+3)}$$

for the calibration $\varepsilon = n^{-1/2}$ dictated by (4.32) when we compare our statistical model with the deterministic perturbation. This is exactly the rate we find in (4.30): the deterministic error model and the statistical error model coincide to that extent.

4.3. Estimating an increment-dependent division rate

Individual dynamics data: a simple renewal problem?

Despite the intricate character of the adder model, which combines the influences of the age and size, in the case where one is given individual dynamics data, the estimate to do is exactly the same as for the pure age-structured model... at least for the genealogical observation case. In

this case, given that we observe a_1, \dots, a_n increments at division, they form a renewal process, observed without bias, and we can apply (4.4) and standard density estimation methods as explained in Section 4.1.

For the population observation case ($k = 2$), things are more intricate: as for the previous models, there exists a selection bias, which is not the same as given by (4.13) since the growth rate of the increment is no more constant and moreover depends on size. However, in the case of exponential growth $\tau(x) = \kappa x$, we have the small miracle already mentioned that $\lambda_2 = \kappa$ and, with $C, C_d > 0$ normalisation constants, we have

$$N_1(a, x) = CxN_2(a, x) \implies f_1(a, x) = C_d x f_2(a, x),$$

where we denote $f_k(a, x)$ the density of dividing cells of increment a and size x . We can thus take advantage of Formula (4.4) and write, for $f_k^a(a) = \int_0^\infty f_k(a, x) dx$ the marginal density along a :

$$B(a) = \frac{f_1^a(a)}{\int_a^\infty f_1^a(s) ds} = \frac{\int_0^\infty f_2(a, x) x dx}{\int_a^\infty \int_0^\infty f_2(s, x) x dx ds}. \quad (4.34)$$

Instead of estimating directly the density $f_2^a(a)$ from the sample (a_1, \dots, a_n) , as done for the genealogical case, one has to estimate a weighted density: from a sample $((A_1, X_1); \dots; (A_n, X_n))$ of increment and size at division of cells according a population observation, we define the following estimate for the debiased density f_1 :

$$\hat{f}_1^a(a) da = K_h * \left(\frac{1}{n} \sum_{i=1}^n X_i \delta_{A_i}(da) \right) = \frac{1}{n} \sum_{i=1}^n X_i K_h(a - A_i) da, \quad (4.35)$$

for which we can prove the same rate of convergence as done for instance in Proposition 4.4.

Population point data: a severely ill-posed problem

When we have treated the case of population point data for the age-structured equation, in Section 4.1, we have remarked that it was rather an instructive toy model than a really interesting case, since if we are able to observe ages in a population, this should mean that we are also able to observe newborn among them, hence dividing cells, hence we would be back to the individual dynamics data.

In the case of the size-structured model, studied in Section 4.2.2 on the contrary, the inverse problem setting appears fully relevant in many experimental cases and different applications - fragmenting polymers, *in vivo* dividing cells, etc.

For the increment model, as for the renewal model, a "naive" inverse problem, which is to assume that we measure samples distributed along a density $N(a, x)$ solution to (3.19) seems irrelevant: observing samples distributed along $N(a, x)$ implies that we also observe newborn, *i.e.* $N(0, x)$, and then why not as well dividing cells - which would bring us back to the individual dynamics data, discussed in the paragraph above.

Much more realistic is the following case, studied in [111]: Assume we are given x_1, \dots, x_n a n -sample of realizations of X_1, \dots, X_n *i.i.d.* random variables of density $N_k^x(x)$ defined by

$$N_k^x(x) := \int_0^\infty N_k(z, x) dz,$$

other said, N_k^x is the x -marginal, or yet the size-distribution of a sample of cells following an increment-structured dynamics, and having reached their steady behaviour given by $N_k(z, x)$. How to estimate an *increment*-dependent division rate $B(a)$ from a *size*-dependent distribution?

Surprisingly, the answer is given by the following proposition, which provides us with a reconstruction formula - and shows that this inverse problem is severely ill-posed.

Proposition 4.10: (*Adapted from Proposition 1 in [111]*) *We have the following reconstruction formula, where \mathcal{F} and \mathcal{F}^{-1} denote the Fourier and inverse Fourier transform:*

$$B(z) = \frac{f(z)}{\int_z^\infty f(s) ds}, \quad f(z) := \mathcal{F}^{-1} \left(\frac{\mathcal{F}[H_1(\cdot)]}{\mathcal{F}[H_1(2\cdot)]} \right),$$

where $H_1(x) = \kappa x \int_0^\infty B(z) x^{k-1} N_k(z, x) dz$ is the solution of the dilation equation given in Proposition 4.8:

$$\mathcal{L}(x) = \frac{\partial}{\partial x} (\kappa x^k N_k) = 2H_1(2x) - H_1(x). \quad (4.36)$$

From this formula, we deduce that if we observe X_1, \dots, X_n an *i.i.d.* sample of law $N_k^x(x)$, we propose the following estimator for B :

$$\widehat{B}_{n,h,h'}(z) = \frac{\widehat{f}_{n,h}(z)}{\widehat{S}_{n,h}(z)} = \frac{\int_{-1/h'}^{1/h'} \frac{\widehat{H_{1,n,h}(\cdot)^*(\xi)}}{\widehat{H_{1,n,h}(\cdot)^*(\xi/2)}} e^{-ia\xi} d\xi}{\int_z^\infty \int_{-1/h'}^{1/h'} \frac{\widehat{H_{1,n,h}(\cdot)^*(\xi)}}{\widehat{H_{1,n,h}(\cdot)^*(\xi/2)}} e^{-is\xi} d\xi ds}$$

where $\widehat{H}_{k,n}$ denotes an approximate solution to the dilation equation (4.36) as seen in Proposition 4.9 with, for the left-hand side,

$$\mathcal{L}_{n,h}(x) := \frac{1}{n} \sum_{i=1}^n \frac{\partial}{\partial x} (\kappa x^k K_h(x - X_i))$$

Proof: As a sketch of the proof in this simpler case where $\tau(x) = \kappa x$ (see [111] for a general growth rate $\tau(x)$) we first write the equation for N_1 , noticing that $N_1 = x^{k-1}N_k$ up to a constant, and integrate it along z to find the dilation equation (4.36). We then solve the equation for $C(z, x) = \kappa x N_1(z, x)$ along the characteristics, and find

$$\kappa x N_1(z, x) = \kappa(x - z)N_1(0, x - z)e^{-\int_0^z B(s)ds}.$$

We use this expression in the definition of H_1 and find

$$H_1(x) = \int_0^x B(z)\kappa x N_1(z, x)dz = \int_0^x B(z)\kappa(x - z)N_1(0, x - z)e^{-\int_0^z B(s)ds}dz$$

using the boundary condition, we also have

$$\kappa x N_1(0, x) = 4\kappa x \int_0^{2x} B(z)N_1(z, 2x)dz = 2H_1(2x)$$

hence

$$H_1(x) = \int_0^x B(z)e^{-\int_0^z B(s)ds}2H_1(2(x - z))dz = f_1 * (2H_1(2\cdot))(x)$$

which appears as a deconvolution problem, where $2H_1(2x)$ plays the role of "noise". \square

We refer to [111] for a thorough numerical investigation.

5. Application to experimental data

In the previous section, we have developed methods to estimate the division rate in three different models: age-structured, size-structured or size-increment-structured model. In the case where data are rich enough, these methods can be used not only to estimate the division rate but also to select which model is more likely. This model selection is carried out here on the case of individual dynamics data: in the case of point population data, estimating the division rate is possible, but the comparison between models is not, since the data is not informative enough.

5.1. Guideline of a protocol

To test a given (age, size or size-increment - or anything else not included in this chapter) model, we

- calibrate it as done in Section 4,

- simulate an age-size or increment-size model, in which our modelling assumption is embedded: see in Section 3.4 the model (2.12)(2.13). For instance, if we want to compare the adder to the sizer without generalising any assumption on the growth rate or on the fragmentation kernel, we can simulate the following model:

$$\frac{\partial}{\partial t} n_k + \frac{\partial}{\partial z} (\kappa x n_k) + \frac{\partial}{\partial x} (\kappa x n_k) = -\kappa x B(z, x) n_k(t, z, x),$$

$$n_k(t, z = 0, x) = 4k \int_0^\infty B(z, 2x) n_k(t, z, 2x) dz$$

till its asymptotic steady behaviour $n_k(t, a, x) = e^{\lambda t} N_k(a, x)$ is reached. This simulation step may be carried out either by using the PDE and an adequate numerical scheme, see for instance [89, 112], or by Monte-Carlo simulations.

- Compare quantitatively data and simulations, by defining a convenient distance between measures. This choice has always some intrinsic arbitrariness and is open to debate. We refer to the paper [113] that discusses Wasserstein distances (and some of their weighted variants), interpreted as connections from univariate methods like the Kolmogorov-Smirnov test, QQ plots and ROC curves, to other multivariate tests. A thorough discussion of statistical tests or distance choices in this context lies beyond the level of generality intended here. We nevertheless refer to [19] where an operational protocol is proposed to compare different division rate models.

5.2. Some results

This protocol has been used in [19] to compare the age-structured and the size-structured equation, compared quantitatively by L^2 norms between regularised solutions. We reproduce in Fig. 10 the sensitivity analysis carried out, which concluded that taking into account the experimental variability in the growth rates (recall Fig. 7 Left) or in the fragmentation kernel b_0 (recall Fig. 7 Right) does not improve significantly the results.

This protocol has then been improved to take into account the adder model, and implemented in the prototype CellDivision platform <https://celldivision.paris.inria.fr/welcome/>, developed by Adeline Fermanian [114]. This platform estimates the three models - age, size or increment structured - when the user provides individual dynamics data of lifetimes, size at birth, size at division and/or increment of size at division,

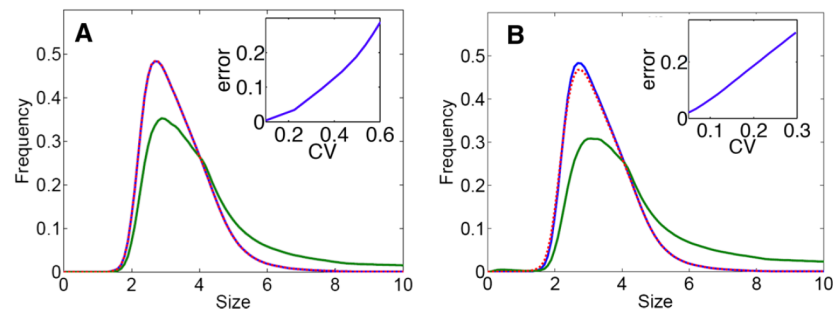


Fig. 10. Effect of adding variability on the size-distribution of cells. A: adding variability in the growth rate, B: in the fragmentation kernel. In green the size distribution with a coefficient of variation of 60%, in dotted pink the simulation without variability, in blue the estimate of the experimental distribution. The insets show the distance between the distribution with no variability and the distance with a variability of given CV: the conclusion is that, for these experiments on bacteria, variability is negligible and the simplified models fit well. Fig. 4 from [19].

together with a growth law. We show on Fig. 11 an application on data from [5] also used in [19], for which it clearly appears that the incremental model fits better.

Of note, a very efficient way of comparing model and data, used in many biophysical papers such as [21, 115], consists in comparing the correlation coefficients between size, age and increment for the various models, since an age model predicts no correlation between size at birth and generation time, and an adder model between size at birth and increment at division. We reproduce in Table 1 the results obtained on genealogical data from [5], comparing experimental correlations with the ones obtained from the calibrated incremental model (using the CellDivision platform): the match is excellent.

Table 1. Correlation coefficients (C.C.) for the data shown in Fig. 11.

AD: Age at Division, SB: Size at Birth, SD: size at Division, ID: Increment at Division. Computed by the CellDivision prototype platform [114].

C.C. between:	AD/SB	AD/SD	AD/ID	SB/SD	SB/ID	SD/ID
Experimental	-0.47	0.53	0.82	0.42	-0.03	0.89
Timer model	-0.02	0.04	0.08	0.98	0.93	0.98
Sizer model	-0.66	0.67	0.92	0.08	-0.39	0.89
Adder model	-0.48	0.51	0.86	0.49	-0.01	0.87

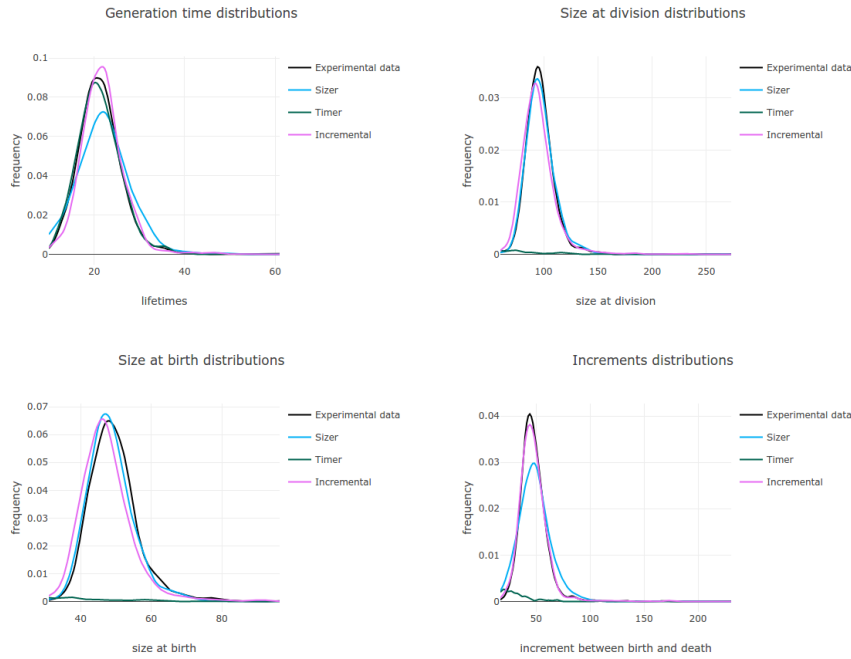


Fig. 11. Screenshot of results obtained by the prototype platform CellDivision, developed by Adeline Fermanian, to fit genealogical data of bacterial division from [5].

6. Perspectives and open questions

In this chapter, we retraced the methods developed by our group during the last decade, originating in [12], to estimate the division rate in linear structured population equation models. They crucially rely on the mathematical analysis of the long-term behaviour of these equations and processes, sketched in Section 3. Many developments still need to be done.

These models are well-adapted to model experiments in a steady environment, typically, with unrestricted nutrient and space. How to estimate the division in a non-steady environment? This could be of tremendous importance to understand for instance how cells react to an external stress, or to take into account cell-to-cell interaction.

We have focused in the chapter on three main models: age-structured, size-structured, and increment-structured model. The method is always the

same, but the mathematical analysis of both the time asymptotics and of the inverse problem is specific. It would be very interesting to adapt it to richer models, for instance taking into account heterogeneity, or the G1/S/G2/M steps in the eucaryotic cell cycle, or yet models structured in DNA content, as the initiation of DNA replication appears to be the true important stage in the life of yeast cells [115] for instance.

The inference methods outlined in Section 4 could be enriched by taking into account other types of noise, in particular adding experimental measurement noise linked to image analysis. They could also lead to the design and study of statistical tests - especially interesting when the data is richer, given by individual dynamics data. In this case, we could also investigate the question of model selection: instead of depending on an *observed* variable, the division rate could depend on a *hidden* variable, more or less in the spirit of Section 4.3 for population point data [111].

Acknowledgments

The content of this note is based on a lecture given at IMS of National University of Singapore in January 2020. The authors thank Professor Weizhu Bao and IMS for providing such a nice opportunity. This work was partially supported by the ERC Starting Grant SKIPPERAD (Grant number 306321).

References

1. M.-C. Duvernoy, T. Mora, M. Ardré, V. Croquette, D. Bensimon, C. Quillet, J.-M. Ghigo, M. Baland, C. Beloin and S. Lecuyer, Asymmetric adhesion of rod-shaped bacteria controls microcolony morphogenesis, *Nature communications*. **9** (2018), 1–10.
2. D. Dell’Arciprete, M. Blow, A. Brown, F. Farrell, J. S. Lintuvuori, A. McVey, D. Marenduzzo, and W. C. Poon, A growing bacterial colony in two dimensions as an active nematic, *Nature communications*. **9** (2018), 1–9.
3. M. Doumic, S. Hecht, and D. Peurichard, A purely mechanical model with asymmetric features for early morphogenesis of rod-shaped bacteria microcolony, *arXiv preprint arXiv:2008.04532*. (2020).
4. N. Q. Balaban, J. Merrin, R. Chait, L. Kowalik, and S. Leibler, Bacterial persistence as a phenotypic switch, *Science*. **305** (2004), 1622–1625.
5. P. Wang, L. Robert, J. Pelletier, W. L. Dang, F. Taddei, A. Wright, and S. Jun, Robust growth of *Escherichia coli*, *Curr. Biol.* **20** (2010), 1099–103.
6. A. Meunier, F. Cornet, and M. Campos, Bacterial cell proliferation: from molecules to cells, *FEMS Microbiology Reviews*. **45** (2021), fuaa046.

7. W.-F. Xue and S. E. Radford, An imaging and systems modeling approach to fibril breakage enables prediction of amyloid behavior, *Biophys. Journal*. **105** (2013), 2811–2819.
8. D. M. Beal, M. Tournus, R. Marchante, T. J. Purton, D. P. Smith, M. F. Tuite, M. Doumic, and W.-F. Xue, The division of amyloid fibrils: Systematic comparison of fibril fragmentation stability by linking theory with experiments, *Iscience*. **23** (2020), 101512.
9. M. Tournus, M. Escobedo, W.-F. Xue, and M. Doumic, Insights into the dynamic trajectories of protein filament division revealed by numerical investigation into the mathematical model of pure fragmentation. (2021), hal-03131754.
10. M. Hoffmann and N. Krell, Statistical analysis of self-similar conservative fragmentation chains, *Bernoulli*. **17** (2011), 395–423.
11. B. Basse, B. Baguley, E. Marshall, W. Joseph, B. van Brunt, G. Wake, and D. J. N. Wall, A mathematical model for analysis of the cell cycle in cell lines derived from human tumors, *J. Math. Biol.* **47** (2003), 295–312.
12. B. Perthame and J. Zubelli, On the inverse problem for a size-structured population model, *Inverse Problems*. **23** (2007), 1037–1052.
13. M. Escobedo, S. Mischler and M. Rodriguez Ricard, On self-similarity and stationary problem for fragmentation and coagulation models, *Annales de l'Institut Henri Poincaré (C) Non Linear Analysis*. **22** (2005), 99–125.
14. M. Hoffmann and A. Olivier, Nonparametric estimation of the division rate of an age dependent branching process, *Stochastic Processes and their Applications*. **126** (2016), 1433–1471.
15. A. W. Van Der Vaart and J. A. Wellner. Weak convergence. In *Weak convergence and empirical processes*, pp. 16–28. Springer, 1996.
16. N. Fournier and A. Guillin, On the rate of convergence in Wasserstein distance of the empirical measure, *Probability Theory and Related Fields*. **162** (2015), 707–738.
17. J. Weed and F. Bach, Sharp asymptotic and finite-sample rates of convergence of empirical measures in Wasserstein distance, *Bernoulli*. **25** (2019), 2620–2648.
18. E. Stewart, R. Madden, G. Paul, and F. Taddei, Aging and death in an organism that reproduces by morphologically symmetric division, *PLoS Biol.* **3** (2005).
19. L. Robert, M. Hoffmann, N. Krell, S. Aymerich, J. Robert, and M. Doumic, Division in *Escherichia coli* is triggered by a size-sensing rather than a timing mechanism, *BMC Biology*. **12** (2014), 17. doi: 10.1186/1741-7007-12-17.
20. A. Amir, Cell size regulation in bacteria, *Phys. Rev. Lett.* **112** (2014), 208102.
21. S. Taheri-Araghi, S. Bradde, J. T. Sauls, N. S. Hill, P. A. Levin, J. Paulsson, M. Vergassola, and S. Jun, Cell-size control and homeostasis in bacteria, *Current Biology*. **11679** (2015), 1–7.
22. F. Si, G. Le Treut, J. T. Sauls, S. Vadia, P. A. Levin, and S. Jun, Mechanistic origin of cell-size control and homeostasis in bacteria, *Current Biology*. **29** (2019), 1760–1770.

23. B. Delyon, B. de Saporta, N. Krell, and L. Robert, Investigation of asymmetry in E. coli growth rate., *Case Studies in Business, Industry & Government Statistics*. **7** (2018).
24. J. Lamperti, Continuous state branching processes, *Bulletin of the American Mathematical Society*. **73** (1967), 382–386.
25. D. G. Kendall, Branching processes since 1873, *Journal of the London Mathematical Society*. **1** (1966), 385–406.
26. T. E. Harris, Branching processes, *The Annals of Mathematical Statistics*. (1948), 474–494.
27. B. A. Sevastyanov, Limit theorems for branching stochastic processes of special form, *Theory of Probability & Its Applications*. **2** (1957), 321–331.
28. P. Haccou, P. Jagers, and V. Vatutin, *Branching processes: variation, growth, and extinction of populations*. Number 5, Cambridge university press, 2005.
29. S. Méléard and V. C. Tran, Trait substitution sequence process and canonical equation for age-structured populations, *Journal of Mathematical Biology*. **58** (2009), 881–921.
30. N. Champagnat, R. Ferrière, and S. Méléard, Unifying evolutionary dynamics: from individual stochastic processes to macroscopic models, *Theoretical population biology*. **69** (2006), 297–321.
31. N. Champagnat, R. Ferrière, and S. Méléard, From individual stochastic processes to macroscopic models in adaptive evolution, *Stochastic Models*. **24** (2008), 2–44.
32. V. Bansaye, J.-F. Delmas, L. Marsalle, and V. C. Tran, Limit theorems for Markov processes indexed by continuous time Galton–Watson trees, *The Annals of Applied Probability*. **21** (2011), 2263–2314.
33. V. Bansaye, M.-E. Caballero, and S. Méléard, Scaling limits of population and evolution processes in random environment, *Electronic Journal of Probability*. **24** (2019), 1–38.
34. B. Perthame, *Transport equations in biology*. Frontiers in Mathematics, Birkhäuser Verlag, Basel, 2007.
35. P. Michel, S. Mischler, and B. Perthame, General relative entropy inequality: an illustration on growth models, *J. Math. Pures Appl. (9)*. **84** (2005), 1235–1260.
36. M. Doumic and P. Gabriel, Eigenelements of a general aggregation-fragmentation model, *Mathematical Models and Methods in Applied Sciences*. **20** (2009), 757.
37. M. Doumic, M. Hoffmann, N. Krell, and L. Robert, Statistical estimation of a growth-fragmentation model observed on a genealogical tree, *Bernoulli*. **21** (2015), 1760–1799.
38. F. Baccelli, B. Błaszczyszyn, and M. Karray. Random measures, point processes, and stochastic geometry, 2020.
39. D. J. Daley and D. Vere-Jones, *An introduction to the theory of point processes: volume I: elementary theory and methods*. Springer, 2003.
40. J. Jacod and A. Shiryaev, *Limit theorems for stochastic processes*. vol. 288, Springer Science & Business Media, 2013.

41. Tran, Viet Chi, Large population limit and time behaviour of a stochastic particle model describing an age-structured population, *ESAIM: PS*. **12** (2008), 345–386.
42. N. Fournier and S. Méléard, A microscopic probabilistic description of a locally regulated population and macroscopic approximations, *The Annals of Applied Probability*. **14** (2004), 1880–1919.
43. J. Bertoin, *Random fragmentation and coagulation processes*. vol. 102, Cambridge University Press, 2006.
44. B. Haas, Loss of mass in deterministic and random fragmentations, *Stochastic processes and their applications*. **106** (2003), 245–277.
45. W. Kermack and A. McKendrick, A contribution to the mathematical theory of epidemics, *Proc. Roy. Society of London, Series A*. **115** (1927), 700–721.
46. J. A. J. Metz and O. Diekmann, eds., *The dynamics of physiologically structured populations*. vol. 68, *Lecture Notes in Biomathematics*, Springer-Verlag, Berlin, 1986. ISBN 3-540-16786-2. Papers from the colloquium held in Amsterdam, 1983.
47. T. E. Harris, *The theory of branching processes*. vol. 6, Springer Berlin, 1963.
48. W. Feller. On the integral equation of renewal theory. In *Selected Papers I*, pp. 567–591. Springer, 2015.
49. J. L. Doob, Renewal theory from the point of view of the theory of probability, *Transactions of the American Mathematical Society*. **63** (1948), 422–438.
50. A. J. Lotka, Application of recurrent series in renewal theory, *The Annals of Mathematical Statistics*. **19** (1948), 190–206.
51. P. Gabriel, Measure solutions to the conservative renewal equation, *ESAIM: Proceedings and Surveys*. **62** (2018), 68–78.
52. P. Gwiazda and E. Wiedemann, Generalized entropy method for the renewal equation with measure data, *Communications in Mathematical Sciences*. **15** (2017), 577–586.
53. P. Gwiazda and B. Perthame, Invariants and exponential rate of convergence to steady state in the renewal equation, *Markov Process. Related Fields*. **12** (2006), 413–424.
54. S. Mischler, B. Perthame, and L. Ryzhik, Stability in a nonlinear population maturation model, *Mathematical Models and Methods in Applied Sciences*. **12** (2002), 1751–1772.
55. V. Bansaye, B. Cloez, and P. Gabriel, Ergodic behavior of non-conservative semigroups via generalized Doeblin conditions, *Acta Applicandae Mathematicae*. (2019), 1–44.
56. S. Mischler and J. Scher, Spectral analysis of semigroups and growth-fragmentation equations, *Annales de l'Institut Henri Poincaré (C) Non Linear Analysis*. **33** (2016), 849–898.
57. W. Feller, *An introduction to probability theory and its applications. Vol. II*. John Wiley and Sons Inc., 1971.
58. P. Gwiazda and B. Perthame, Invariants and exponential rate of convergence to steady state in the renewal equation., *Markov Processes and Related*

- Fields*. **2** (2006), 413–424.
59. V. Bansaye and V. C. Tran, Branching Feller diffusion for cell division with parasite infection, *ALEA, Lat. Am. J. Probab. Math. Stat.* **8** (2011), 95–127.
 60. V. Bansaye, Proliferating parasites in dividing cells: Kimmel’s branching model revisited, *Ann. Appl. Probab.* **18** (2008), 967–996.
 61. B. Cloez, Limit theorems for some branching measure-valued processes, *Advances in Applied Probability*. **49** (2017), 549–580.
 62. O. Diekmann, H. Heijmans, and H. Thieme, On the stability of the cell size distribution, *Journal of Mathematical Biology*. **19** (1984), 227–248.
 63. O. Diekmann, M. Gyllenberg, and J. Metz, Steady-state analysis of structured population models, *Theoretical population biology*. **63** (2003), 309–338.
 64. M. Escobedo, A short remark on a growth–fragmentation equation, *Comptes Rendus Mathématique*. **355** (2017), 290–295.
 65. M. Doumic and B. Van Brunt, Explicit solution and fine asymptotics for a critical growth-fragmentation equation, *ESAIM: Proceedings and Surveys*. **62** (2018), 30–42.
 66. T. Suebcharoen, B. Van Brunt, and G. Wake, Asymmetric cell division in a size-structured growth model, *Differential and Integral Equations*. **24** (2011), 787–799.
 67. P. Michel, Existence of a solution to the cell division eigenproblem, *Math. Models Methods Appl. Sci.* **16** (2006), 1125–1153.
 68. P. Michel, S. Mischler, and B. Perthame, General entropy equations for structured population models and scattering, *C. R. Math. Acad. Sci. Paris*. **338** (2004), 697–702.
 69. M. J. Cáceres, J. A. Cañizo, and S. Mischler, Rate of convergence to an asymptotic profile for the self-similar fragmentation and growth-fragmentation equations, *Journal de mathématiques pures et appliquées*. **96** (2011), 334–362.
 70. N. Fournier and B. Perthame, A non-expanding transport distance for some structured equations, *arXiv preprint*.
 71. J. A. Cañizo, P. Gabriel, and H. Yoldaş, Spectral gap for the growth-fragmentation equation via Harris theorem, *arXiv preprint arXiv:2004.08343*. (2020).
 72. E. Bernard and P. Gabriel, Asymptotic behavior of the growth-fragmentation equation with bounded fragmentation rate, *Journal of Functional Analysis*. **272** (2017), 3455–3485.
 73. D. Balagué, J. Cañizo, and P. Gabriel, Fine asymptotics of profiles and relaxation to equilibrium for growth-fragmentation equations with variable drift rates, *Kinetic and related models*. **6** (2013), 219–243.
 74. J. Bertoin, On a Feynman-Kac approach to growth-fragmentation semi-groups and their asymptotic behaviors, *Journal of Functional Analysis*. **277** (2019), 108270.
 75. J. Bertoin and A. R. Watson, The strong malthusian behavior of growth-fragmentation processes, *Annales Henri Lebesgue*. **3** (2020), 795–823.
 76. B. Haas. Regularity of formation of dust in self-similar fragmentations. In *Annales de l’IHP Probabilités et statistiques*, vol. 40, pp. 411–438, 2004.

77. B. Haas, Asymptotic behavior of solutions of the fragmentation equation with shattering: an approach via self-similar Markov processes, *Annals of Applied Probability*. **20** (2010), 382–429.
78. C. Goldschmidt and B. Haas, Behavior near the extinction time in self-similar fragmentations i : the stable case, *Annales de l'I.H.P. Probabilités et statistiques*. **46** (2010), 338–368. doi: 10.1214/09-AIHP317.
79. P. Dyszewski, N. Gantert, S. G. Johnston, J. Prochno, and D. Schmid, Sharp concentration for the largest and smallest fragment in a k -regular self-similar fragmentation, *arXiv preprint arXiv:2102.08935*. (2021).
80. C. Goldschmidt, and B. Haas, Behavior near the extinction time in self-similar fragmentations ii: Finite dislocation measures, *Annals of Probability*. **44** (2016), 739–805.
81. J. Banasiak, Shattering and non-uniqueness in fragmentation models; an analytic approach, *Physica D: Nonlinear Phenomena*. **222** (2006), 63–72.
82. J. Banasiak, W. Lamb, and P. Laurençot, *Analytic Methods for Coagulation-Fragmentation Models, Volume I*. CRC Press, 2019.
83. M. Doumic and M. Escobedo, Time asymptotics for a critical case in fragmentation and growth-fragmentation equations, *Kinetic & Related Models*. **9** (2016), 251.
84. M. Escobedo. On the non existence of non negative solutions to a critical growth-fragmentation equation. In *Annales de la Faculté des sciences de Toulouse: Mathématiques*, vol. 29, pp. 177–220, 2020.
85. J. Bertoin and A. R. Watson, Probabilistic aspects of critical growth-fragmentation equations, *Advances in Applied Probability*. **48** (2016), 37–61.
86. G. Greiner and R. Nagel. Growth of cell populations via one-parameter semigroups of positive operators. In *Mathematics applied to science*, pp. 79–105. Elsevier, 1988.
87. E. Bernard, M. Doumic, and P. Gabriel, Cyclic asymptotic behaviour of a population reproducing by fission into two equal parts, *Kinetic and Related Models*. **12** (2019), 551.
88. P. Gabriel and H. Martin, Periodic asymptotic dynamics of the measure solutions to an equal mitosis equation, *arXiv preprint arXiv:1909.08276*. (2019).
89. J. A. Carrillo, P. Gwiazda, and A. Ulikowska, Splitting-particle methods for structured population models: convergence and applications, *Mathematical Models and Methods in Applied Sciences*. **24** (2014), 2171–2197.
90. V. Bansaye and S. Méléard, *Stochastic models for structured populations*. vol. 16, Springer, 2015.
91. P. Gwiazda, T. Lorenz, and A. Marciniak-Czochra, A nonlinear structured population model: Lipschitz continuity of measure-valued solutions with respect to model ingredients, *Journal of Differential Equations*. **248** (2010), 2703–2735.
92. P. Gabriel and H. Martin, Steady distribution of the incremental model for bacteria proliferation, *arXiv preprint arXiv:1803.04950*. (2018).
93. M. Doumic, Analysis of a population model structured by the cells molecular content, *Math. Model. Nat. Phenom.* **2** (2007), 121–152.

94. H. Kang, X. Huo, and S. Ruan, Nonlinear physiologically structured population models with two internal variables, *Journal of Nonlinear Science*. **30** (2020), 2847–2884.
95. H. Banks, K. Sutton, W. Thompson, G. Bocharov, D. Roosec, T. Schenkeld, and A. Meyerhanse, Estimation of cell proliferation dynamics using cfse data, *Bull. of Math. Biol.* (2010).
96. A. B. Tsybakov, *Introduction à l'estimation non paramétrique*. vol. 41, Springer Science & Business Media, 2003.
97. E. Giné and R. Nickl, *Mathematical foundations of infinite-dimensional statistical models*. Cambridge University Press, 2021.
98. M. Hoffmann and A. Olivier, Statistical analysis for structured models on trees, *Statistical Inference for Piecewise-deterministic Markov Processes*. (2018), 1–38.
99. M. Doumic, M. Hoffmann, P. Reynaud, and V. Rivoirard, Nonparametric estimation of the division rate of a size-structured population, *SIAM J. on Numer. Anal.* **50** (2012), 925–950.
100. M. Nussbaum and S. Pereverzev, The degrees of ill-posedness in stochastic and deterministic noise models, *Preprint WIAS 509*. (1999).
101. M. Doumic, B. Perthame, and J. Zubelli, Numerical solution of an inverse problem in size-structured population dynamics, *Inverse Problems*. **25** (2009), 045008.
102. M. Doumic, M. Escobedo, and M. Tournus, Estimating the division rate and kernel in the fragmentation equation, *Annales de l'Institut Henri Poincaré (C) Non Linear Analysis*. **35** (2018), 1847–1884.
103. V. H. Hoang, T. M. Pham Ngoc, V. Rivoirard, and V. C. Tran, Nonparametric estimation of the fragmentation kernel based on a partial differential equation stationary distribution approximation, *Scandinavian Journal of Statistics*. (2020), 1–40.
104. M. Hairer and J. C. Mattingly. Yet another look at Harris' ergodic theorem for Markov chains. In *Seminar on Stochastic Analysis, Random Fields and Applications VI*, pp. 109–117, 2011.
105. P. H. Baxendale, Renewal theory and computable convergence rates for geometrically ergodic Markov chains, *The Annals of Applied Probability*. **15** (2005), 700–738.
106. S. V. B. Penda, M. Hoffmann, and A. Olivier, Adaptive estimation for bifurcating Markov chains, *Bernoulli*. **23** (2017), 3598–3637.
107. H. Engl, M. Hanke, and A. Neubauer, *Regularization of inverse problems*. vol. 375, *Mathematics and its Applications*, Springer, 1996.
108. T. Bourgeron, M. Doumic, and M. Escobedo, Estimating the division rate of the growth-fragmentation equation with a self-similar kernel, *Inverse Problems*. **30** (2014), 025007.
109. G. Wahba, Practical approximate solutions to linear operator equations when the data are noisy, *SIAM journal on numerical analysis*. **14** (1977), 651–667.
110. M. Nussbaum, Asymptotic equivalence of density estimation and Gaussian white noise, *The Annals of Statistics*. (1996), 2399–2430.

111. M. Doumic, A. Olivier, and L. Robert, Estimating the division rate from indirect measurements of single cells., *Discrete & Continuous Dynamical Systems-Series B*. **25** (2020).
112. J. A. Carrillo, P. Gwiazda, K. Kropielnicka, and A. K. Marciniak-Czochra, The escalator boxcar train method for a system of age-structured equations in the space of measures, *SIAM Journal on Numerical Analysis*. **57** (2019), 1842–1874.
113. A. Ramdas, N. G. Trillos, and M. Cuturi, On Wasserstein two-sample testing and related families of nonparametric tests, *Entropy*. **19** (2017), 47.
114. A. Fermanian, C. Doucet, M. Hoffmann, L. Robert, and M. Doumic, Celldivision: a platform to select a best-fit cell division cycle model. In progress, prototype platform available at <https://celldivision.paris.inria.fr/welcome/>.
115. I. Soifer, L. Robert, and A. Amir, Single-cell analysis of growth in budding yeast and bacteria reveals a common size regulation strategy, *Current Biology*. **26** (2016), 356–361.